UNIVERSITY OF BAYREUTH - MICROMETEOROLOGY

BACHELOR THESIS

Changes in Precipitation Distribution and Intensity and their Consequences on Water Balance in the Fichtelgebirge, Northern Bavaria

Tino Schneidewind
1713020

supervised by
Dr. Wolfgang Babel
Prof. Dr. Christoph Thomas

Bayreuth, May 3rd, 2023

Acknowledgements

I wish to thank Mona and Tuuli for providing me with love and happiness during this work-intensive time. Thank you for forcing me off my laptop and taking me into nature, even though most of the time it was freezing.

I am very grateful for having had Wolfgang Babel as my primary supervisor. He always took the time to discuss my thesis and help me with my problems. Many thanks to Christoph Thomas and the whole Micrometeorology Group for asking the right questions and supplying me with inspiration and ideas.

Lastly, I wish to thank my parents and grandparents for supporting me financially during my studies. Without them, I would never have had the chance to write this thesis.

Thank you,
Tino

Abstract

In the age of climate change, global warming enhances the atmosphere's ability to take up water vapor (Collins et al., 2013). Consequently, evapotranspiration rates globally are rising, leading to an amplified drought potential, as well as an increase in global annual precipitation (Trenberth, 2011; Dunn et al., 2020). With rising temperature, extreme precipitation has risen in intensity and occurrence (Zhang and Zhou, 2019). However, the local representation of these global trends depends on characteristics like topography and continentality (Łupikasza, 2016). In the Fichtelgebirge, there has been no detailed investigation of extreme precipitation, although there has been extensive research on the effects of climate change. This thesis investigated precipitation and water balance trends, and focussed on the bias of extreme precipitation events from 1994-2022. In line with the global trend, we hypothesized that extreme precipitation would increase, while water balance would decrease. To detect extreme precipitation, precipitation indices, event analysis and subdaily analysis were used, while assuming the two latter to be crucial for a precise determination of extreme precipitation trends. The data has shown, that precipitation and water balance significantly declined over the observation period, mainly in spring and summer. Extreme precipitation displayed declining trends. However, subdaily and event analysis would not have been necessary to detect this trend in this case. Interestingly, a nearby weather station outside the mountain range experienced no decline in extreme precipitation. The data suggests, that the potential for droughts could rise in the future, as water availability decreases in the growing season and the water table lowers.

Zusammenfassung

Durch die globale Erderwärmung kann die Atmosphäre kontinuierlich mehr Wasserdampf aufnehmen (Collins et al., 2013). Dadurch haben Evapotranspirationsraten zugenommen, welche das Dürrepotential steigern (Trenberth, 2011). Außerdem nimmt die globale jährlich Niederschlagsmenge zu (Dunn et al., 2020). Mit der steigenden Temperatur haben auch die Anzahl und die Intensität von Extremniederschlagsereignissen zugenommen (Zhang and Zhou, 2019). Jedoch hängt die lokale Auswirkung dieser globalen Trends von Standorteigenschaften wie der Topographie und Kontinentalität ab (Łupikasza, 2016). Im Fichtelgebirge wurde die Entwicklung der Extremniederschläge noch nicht detailliert untersucht, obwohl bereits viele Studien zu den Auswirkungen des Klimawandels durchgeführt wurden. In dieser Arbeit wird die Tendenz des Niederschlag und der Wasserbilanz zwischen 1994-2022 bestimmt, und untersucht, ob Extremniederschläge Trends aufweisen. Gemäß dem globalen Mittel wurde erwartet, dass Extremniederschläge zunehmen und die Wasserbilanz abnimmt. Zur genauen Bestimmung von Extremniederschlägen wurden Niederschlagsindizes auf Tagesdatenbasis und Eventanalyse mithilfe von 10-Minuten Daten verwendet. Dabei wurde angenommen, dass die 10-Minuten Daten ein genaueres Bild der Extremniederschlagstrends abbilden. Die Messungen haben ergeben, dass der Niederschlag und die Wasserbilanz signifikant über den Beobachtungszeitraum abgenommen haben, hauptsächlich im Frühling und Sommer. Auch die Extremniederschläge haben abgenommen, aber die 10-Minuten Daten wären in unserem Fall nicht nötig gewesen um diese Trends zu Bestimmen. Die Ergebnisse implizieren, dass es in Zukunft einen Anstieg des Dürrepotentials geben könnte, durch die Verringerung der Wasserverfügbarkeit in der Wachstumsperiode der Vegetation und einer Absenkung des Grundwasserspiegels des Einzugsgebietes. Ein Vergleich mit einer nahegelegenen Wetterstationen hat ergeben, dass die Abnahme der Extremereignisse die Folge der spezielle Topographie des Mittelgebirges sein könnte, da dort keine abnehmenden Trends festgestellt wurden.

Contents

Acknowledgements **I**

Abstract **III**

Zusammenfassung **V**

1 Introduction **1**
1.1 Motivation 1
1.2 Global climate change trends 1
1.3 Climate change in northern Bavaria 3
1.4 Objectives 4

2 Methods **5**
2.1 Site description 5
2.2 Observations 6
2.3 Precipitation analysis 6
2.4 Evapotranspiration modeling with Penman-Monteith 7
2.5 Data processing and gap filling 8

3 Results **11**
3.1 Precipitation trends 11
3.2 Water balance 14
3.3 Indices of precipitation 17
3.4 Precipitation events and intensities 21

4 Discussion **24**
4.1 Why did precipitation and water balance decrease? 24
4.2 Why did extreme precipitation reduce? 25
4.3 Is sub daily analysis of extreme precipitation necessary? 27
4.4 Did the Waldstein climate dry over time? 27
4.5 Why did evapotranspiration decline? 28
4.6 Do we face a rapid temperature increase? 30

5 Conclusion **31**

Bibliography **32**

Declaration **36**

Appendix **37**

List of Figures

1 Aerial view of the Lehstenbach catchment (19.04.2015), ©Google Earth 2015, MT: Main Tower, TT: Turbulence Tower 5
2 Data availability for 10-minute precipitation data, daily precipitation data, modeled evapotranspiration, and calculated water balance data. 9
3 Averages of monthly precipitation (left) and temperature (right) with arrows as standard deviations from 1994 to 2022. 11
4 Annual precipitation from 1994 to 2022. (trend: p=0.004, slope m=-9.3 mm/year). 12
5 Seasonal precipitation sums from 1994 to 2022. (summer trend: p=0.013, m=-4.9). 13
6 Monthly means of evapotranspiration (left) and water balance (right). . . . 14
7 Yearly sum of evapotranspiration. (trend: p=0.01, m=-3.51) 15
8 Seasonal evapotranspiration. (trend summer: p=0.057, m=-2.5 , trend autumn: p=0.050, m=-0.35) 15
9 Yearly water balance. (trend: p=0.01, m=-8.9) 16
10 Seasonal water balance. (trend MAM: p=0.04, m=-3.3) 17
11 Number of wet days NWD with precipitation above 1 mm per day. (trend: p=0.007, m=-0.9). 18
12 Number of wet days per year against annual precipitation. (correlation p=0.000). 18
13 Consecutive dry days CDD (left) and consecutive wet days CWD (right). . 19
14 Maximum precipitation fallen over one day RX1day (left) and 5 days RX5day (right) per year. (trend RX1day: p=0.001, m=-0.73). 19
15 Precipitation fallen above the 95th percentile R95p (left) and 99th percentile R99p (right). (trend R95p: p=0.0002, m=-3.1; trend R99p: p=0.0001, m=-1.1). 20
16 Number of days with precipitation greater than 10 mm per year R10 (left) and 20 mm per year R20 (right). (trend R10: p=0.050 , m=-0.37. trend R20: p= 0.040 , m=-0.19) 21
17 Average monthly precipitation intensity (left). Yearly mean precipitation intensity (right). 22
18 Mean event intensity (left) and maximum event intensity (right). (trend left: p=0.010, m=-0.002. trend right: p=0.015, m=-0.006). 22
19 Yearly 95th percentile of maximum event intensity (left). (trend: p=0.008, m=-0.02). Number of events per year (right). (no trend for 2004-2022) . . 23
20 Maximum 10-minute precipitation intensity per year (left). (Trend: p=0.03, m=-0.12). Annual precipitation fallen above the threshold of 5mm/10min (right). (Trend: p=0.025, m=-1.2). 23

21 Bayreuth: Precipitation fallen above the 95th perventile (left) and above the 99th percentile (right). 26
22 Bayreuth: Number of consecutive wet days (left) and number of consecutive dry days (right) with significant trends. 28
23 Left: Relation between vapor pressure deficit VPD and evapotranspiration according to Penman-Monteith, when measurements of net radiation were above 600 W/m^{-2}. Right: Measurements of wind speeds u per year when measurements of net radiation were above 600 W/m^{-2}. 29
24 Annual mean temperature. (trend: p=0.0003, m=0.06). 39
25 Monthly precipitation. (summer trend: p=0.002, m=-3.0) 40
26 Hydrological seasonal precipitation. 41
27 Hydrological seasonal evapotranspiration. (trend summer: p=0.025, m=-2.27 , trend autumn: p=0.046, m=-1.16) 42
28 Monthly evapotranspiration. (trend May: p=0.03, m=-0.6, trend June: p=0.049, m=-0.77, trend July: p=0.009, m=-0.90, trend August: p=0.009, m=-0.89) 43
29 Hydrological seasonal water balance. 44
30 Monthly water balance. (trend July: p=0.049, m=-2.39) 45
31 Yearly 95th precipitation percentile (left) and 99th precipitation percentile (right) of daily precipitation. (99th trend: p=0.006, m=-0.36). 46
32 Monthly averages of precipitation intensity. (April trend: p=0.014, m=0.004) 47
33 Maximum event intensity distribution per year. 48
34 Number of events with event precipitation sum below 1 mm, 1-5 mm, 5-10 mm, 10-20 mm, 20-30 mm and above 30 mm. No trends for 2004-2022. . . 48
35 Validation of Penman Monteith Model with Eddy-Covariance data with diurnal means of seasons and months. 49
36 Bayreuth: Number of precipitation days with more then 10 mm of precipitation (left) and 20 mm of precipitation (right) with statistically significant trends. 50
37 Bayreuth: Maximum precipitation intensity for each year (left) and precipitation with intensity greater then 5 mm fallen in a year (right) 50
38 Bayreuth: number of wet days per year with significantly decreasing trend. 51
39 Bayreuth: 95th percentile of precipitation intensity (left) and number of events per year (right) with a significant trend. 51

List of Tables

1 Pflanzgarten Instrumentation 6
2 Weidenbrunnen Instrumentation 6
3 Precipitation Indices 7

4 Site Specific Parameters 9

1 Introduction

1.1 Motivation

The purpose of this thesis is to identify precipitation variability in the Fichtelgebirge in Upper Franconia, Germany, in the context of global climate change.
Although Upper Franconia experienced less temperature rise than surrounding regions and no increase in annual precipitation (Foken and Lüers, 2013, 2015), little is known about precipitation intensification and its consequences for water balance. Decades ago, the Fichtelgebirge showed no increase in extreme precipitation, as it is the case globally on average (Foken, 2003). Because of the impact extreme weather events can have on society like in Ahrweiler in 2021, it is vital to update past conclusions.

1.2 Global climate change trends

Continuous fossil fuel combustion leads to growing atmospheric carbon dioxide concentrations (Keeling et al., 1976). Carbon dioxide is a greenhouse gas, meaning it absorbs longwave terrestrial radiation (Tyndall, 1861). Hence, Earth's temperature rises with increasing carbon dioxide concentrations (Foote, 1856). Earth's climate is constantly changing (Latif and Barnett, 1994). However, the current change in regional climate systems can only be explained by anthropogenic factors (Rosenzweig et al., 2008). According to Osborn et al. (2021), the global mean land warming is 1.7 °C since 1860.

Temperature and water vapor are closely connected. The maximum amount of water vapor an air parcel can take up increases by 7% K^{-1}. This relationship is described in the Clausius Clapeyron equation (Trenberth et al., 2003). Evapotranspiration, transitioning of water from a liquid to a gaseous phase, requires energy. This energy is provided by solar radiation, which heats the surface. Evapotranspiration receives energy out of the enthalpy of the surface and consequently cools the surface. As a result, evapotranspiration is limited by the availability of water and energy (Allen and Ingram, 2002).
Both dependencies accelerate evapotranspiration in a warming climate, as relative humidity reduces with rising temperature. Consequently, the risk for droughts is amplified as more water evapotranspires, especially in water-limited regions (Trenberth, 2011). Additionally, water vapor is a greenhouse gas and, therefore, strengthens accelerated evapotranspiration rates, because of its radiative forcing (Scheff and Frierson, 2014). The impact of this positive feedback loop in the global climate system is a crucial part of climate predictions and is to some degree still uncertain.

Evapotranspiration supplies the atmosphere with precipitable water. Precipitable water increases in a warming climate, as the atmosphere can hold more water vapor. Consequently, precipitation increases. This affects surface water balance, which is estimated as

precipitation minus evapotranspiration. In contrast to evapotranspiration, precipitation heats the atmosphere (Allen and Ingram, 2002). Precipitation relies on evapotranspiration and therefore is limited by the energy budget (Pall et al., 2007). Hence, the observed and modeled increase in global mean precipitation is only $1-3\%\ K^{-1}$ (Dunn et al., 2020; Collins et al., 2013). However, precipitation is a high spatial and temporal variable, leading to different trends determined by latitude, continentality, topography, vegetation, and elevation (Łupikasza, 2016).

Overall, there is a change in precipitation patterns. Evidence is building, that the contrast between wet and dry seasons or weather regimes is increasing (Schurer et al., 2020). While global mean precipitation rises relatively slowly, daily extremes are expected to intensify at $7\%\ K^{-1}$, and hourly extremes at an even higher rate (Zhang and Zhou, 2019). This trend towards more intense precipitation influences water balance and subsequently soil water content, as more precipitation is lost to runoff. This change in frequency induces stress and therefore decreases the primary production of existing plants, lowering CO2 fixation (Knapp et al., 2002). Additionally, sustained heavy precipitation can lead to flooding, causing humanitarian and ecological damage (Guzzetti et al., 2005).

According to Łupikasza (2016), extreme precipitation events are defined by their scarcity in a corresponding region. Whether an event qualifies as rare can be determined with relative indices (e.g. 95th percentile), or absolute thresholds (e.g. 20 $mm\ day^{-1}$). Rising extreme precipitation trends are driven by thermodynamic and dynamic effects. Precipitation intensifies due to increased water vapor abundance thermodynamically. Latent heating can enhance storm produced precipitation in large-scale dynamic systems, like the North Atlantic Oscillation (Zhang and Zhou, 2019). Those changes in dynamics can intensify precipitation events above the projected rate of $7\%\ K^{-1}$. Additionally, changes in cloud microphysics can alter the characteristics of extreme precipitation in a warming climate (Sui et al., 2020).

Previous research has established that the average maximum 1-day precipitation has substantially risen over land since 1950. Furthermore, precipitation from days above the 95th percentile has significantly increased all over the globe (Dunn et al., 2020). Maximum annual precipitation in a 5-day period accelerated at a similar rate to 1-day precipitation globally (Zhang and Zhou, 2019), although few studies have investigated this so far. There has been little quantitative analysis of long-term changes in sub-daily extreme precipitation on a planetary scope. However, on a regional scale, sub-daily extreme precipitation has been researched. In Europe, annual maximum 1- and 5-day precipitation has increased since 1950 (Sun et al., 2021), and 5-, 10- and 20-year extreme events have increased in frequency (van den Besselaar et al., 2012). It has been observed that the rise in frequency is mainly in summer and winter (Helama et al., 2018). Although there can

be large differences between regions (Casanueva et al., 2014). Future projections show an increase in precipitation extremes and their frequency is very likely in Europe (Collins et al., 2013). This trend is expected to be amplified in urbanized areas (Georgescu et al., 2021).

1.3 Climate change in northern Bavaria

To date, several studies have investigated climate change in Upper Franconia. Upper Franconia is a region in north-eastern Bavaria, which has been less affected by growing climate risks compared to surrounding lowlands, because of its elevation (Foken and Lüers, 2015). Extensive research has shown that there has been a temperature increase of 0.36 K per decade, in Bayreuth (Upper Franconia), in the last 50 years in comparison to 1961-1990 (Foken and Lüers, 2015). This exceeds the global temperature increase as the global average increase in surface temperature was only 2.7 K per decade (1979-2012) (Stocker, 2014).
Furthermore, there is a trend towards more precipitation in winter and autumn, and less in spring in the Fichtelgebirge, while the annual sum has no significant trend (Lüers et al., 2017). The transition to dryer late winters and early summers influences the water balance leading to reduced water availability because less water is available for plants in their growing season. Additionally, periods of little to no precipitation in Bayreuth are often interrupted by heavy rain and snowfall causing flooding and runoffs, resulting overall in a lowering ground water table (Foken and Lüers, 2015). Foken and Lüers (2013) hypothesized that the frequency and amplitude of extreme weather events will rise in Upper Franconia in the future. However, Upper Franconia is topographically complex, which can lead to high spatiotemporal variability of meteorological parameters (Beniston et al., 2018).

The Fichtelbebirge is a low mountain range, which has been researched intensively in the past. Previous research has established that there is a non-significant trend towards higher annual precipitation. Characteristically for mountainous regions, precipitation in the Fichtelgebirge increases with elevation, especially in winter. The Fichtelgebirge has its primary seasonal precipitation maximum in winter and its secondary in summer. This shift in seasonal distribution influences surface water balance in Upper Franconia, leading to an overall decline despite high annual precipitation sums of 1.162 mm (Lüers et al., 2017; Foken, 2003). As a result, Upper Franconia is highly sensitive to rising evapotranspiration. In contrast to extreme precipitation trends in Europe, the Fichtelgebirge experienced no increase in extreme precipitation (Foken, 2003). However, there has been no detailed investigation of sub-daily extreme precipitation in the Fichtelgebirge.

1.4 Objectives

This bachelor's thesis traces the development of changing precipitation and water balance distributions of the most recent climatological period in the Fichtelgebirge. It assesses the significance of water balance and precipitation trends and determines the tendency of extreme precipitation and precipitation intensity.
In line with these objectives, we hypothesize, that [i] water balance decreases over the years, because of increasing annual evapotranspiration and stable annual precipitation as observed by Lüers et al. (2017). [ii] Water availability declines as a result of a seasonal shift in precipitation (Foken and Lüers, 2015) and potentially evapotranspiration. [iii] Precipitation intensity increases statistically significantly coherently to the global mean, as suggested by Foken and Lüers (2013) and [iiii] precipitation frequency decreases with longer periods of no rain, due to the intensification without an annual increase. Lastly, [iiiii] sub-daily analysis of precipitation is vital to detect changes in extreme and intense precipitation, because of its higher resolution.
The additional decade of climate data compared to past studies enables better long-term predictions and potentially refutes conclusions, which are in hindsight based on precipitations' high temporal variability.

These hypotheses were investigated using data provided by the measurement site at the Waldstein in the Fichtelgebirge. Precipitation was analyzed through indices, sub-daily analysis and event analysis. Evapotranspiration was modeled using the Penman-Monteith approach and used for calculating water balance. Precipitation data was visualized in bar plots and discussed afterwards.

2 Methods

2.1 Site description

The Waldstein measurement site is located in the Fichtelgebirge, a low mountain range in northern Bavaria, Germany. The site is located inside the Lehstenbach catchment (see figure 1) between the Großer Waldstein (879 m above sea level (asl)) and the Bergkopf (857 m asl). All measurements were taken at the Pfanzgarten site (765 m asl, 50°08'35"N, 11°51'49"E)) and the Weidenbrunnen site (775 m asl). The onsite vegetation is mown grass meadow for Pflanzgarten and a spruce forest for Weidenbrunnen. Both sites are separated by 200 m. Climatic observations were done at the Pflanzgarten site and flux measurements at the Weidenbrunnen site. Both sites were set up by the Bayreuth Institute of Terrestrial Ecosystem Research (BITÖK) and operated by the Department of Micrometeorology (University of Bayreuth) since 2004.
The Fichtelgebirge is a densely forested, plutonic, low mountain range with heights up to 1053 m asl at the Schneeberg, which does not reach the timberline. Upper Franconia's climate is influenced by the Atlantic Ocean to the west, as well as the more continental east, and can be classified as humid continental (Foken, 2007). The region received mean annual precipitation of 1.162 mm and had an average temperature of 5.3 K between 1971-2000 (Foken, 2003). Due to the mountain ridge location, the Lehstenbach catchment experiences either an advective relief-rainfall, orographic-lift effect or convective-induced precipitation (Lüers et al., 2017).

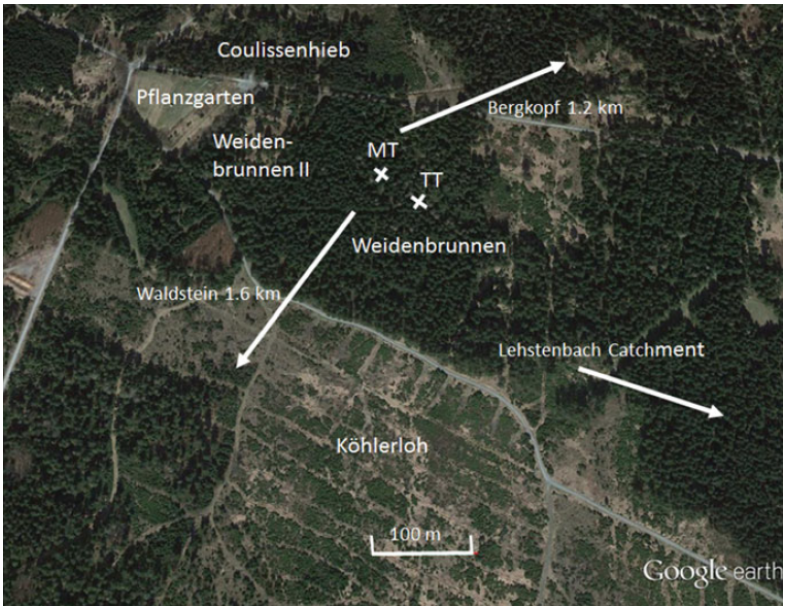

Figure 1: Aerial view of the Lehstenbach catchment (19.04.2015), ©Google Earth 2015, MT: Main Tower, TT: Turbulence Tower

2.2 Observations

The Pflanzgarten site is a forest clearing and was set up in 1994. It is a forest climate station suitable for long term climate measurements. Mainly, temperature and precipitation data were used, although vapor pressure, relative humidity, air pressure, incoming shortwave radiation, and wind velocity measurements were measured to fill in missing data from the Weidenbrunnen site (see table 1). All measurements necessary for the Penman-Monteith evapotranspiration model were taken at the Weidenbrunnen site using the measurement tower, where the canopy was used as the balancing surface (see table 2). The Weidenbrunnen site was set up in 1998.

Table 1: Pflanzgarten Instrumentation

Measurement parameter [unit]	Instrument	Hight (m)
precipitation $[mm]$	Observator Instruments OMC 212	1
precipitation $[mm]$ (2012 onward)	Ott Pluvio^2 (II)	1
air temperature $[°C]$	HMP45, PT 100	2
air pressure $[hPA]$	Ammonit AB60	0
relative humidity [%]	HMP45, capacitive	2
wind velocity $[ms^{-1}]$	Thies cup anemometer	10
incoming shortwave radiation $[W\ m^{-2}]$	EQ07	4

Table 2: Weidenbrunnen Instrumentation

Measurement parameter [unit]	Instrument	Hight (m)
incoming shortwave radiation $[W\ m^{-2}]$	Kipp and Zonen CM 14	30
incoming longwave radiation $[W\ m^{-2}]$	Kipp and Zonen CG 2	30
outgoing shortwave radiation $[W\ m^{-2}]$	Kipp and Zonen CM 14	30
outgoing longwave radiation $[W\ m^{-2}]$	Kipp and Zonen CG 2	30
soil moisture [%]	TDR	-0.1
air temperature $[°C]$	HMP45, PT 100	31
air temprature (wet)$[°C]$	Frankenberger Psychrometer PT100	31
relative humidity [%]	HMP45, capacitive	31
wind velocity $[ms^{-1}]$	Friedrich cup anemometer	32
wind velocity $[ms^{-1}]$	Thies 2D ultrasonic	32
sonic temperature $[ms^{-1},° C]$	Gill 3D-ultrasonicR3-50	33

All meteorological measurements were taken according to standards by the World Meteorological Organisation. Measurements were taken in 10 min intervals. All meteorological parameters were averaged to larger intervals, except precipitation which was summed up.

2.3 Precipitation analysis

Additionally to analyzing precipitation sums of different interval lengths, precipitation indices were calculated from daily sums of precipitation. These indices were introduced

by the Expert Team on Climate Change Detection and Indices (ETCCDI) to ensure comparability between studies concerning climate change and extreme climate (see table 3). Indices that describe extreme precipitation have their units either in mm or days. Volumetric indices like RXday1 and RXday5 are used to describe the most extreme events over a year. Volumetric indices focus on the distribution of annual precipitation like R95p and p95th giving insight into the general trajectory of extreme precipitation in the context of the overall precipitation. Lastly, R10 and R20, count the days with precipitation over their respective threshold, therefore depicting a clear trend of occurrence for future events of that intensity.

In addition to indices, precipitation was analyzed using event analysis. Precipitation events were separated by a measurement interval of 10 min, which did not detect any precipitation with a threshold of 0.1 mm. Compared to daily analysis of precipitation, this enables a clear analysis of changing weather patterns. Additionally, analysis was done with 10 min data without accounting for events.

For seasonal analysis of trends, two definitions were used. Hydrologically, where winter spans from November to January and summer from May to July. Meteorologically, where winter spans from December to February, and summer from June to August.

Table 3: Precipitation Indices

ID	Definition	Unit
RX1day	maximum 1-day precipitation	mm
RX5day	maximum 5-day precipitation	mm
R95p	annual total precipitation from days >95th% percentile	mm
R99p	annual total precipitation from days >99th% percentile	mm
p95th	95th percentile of daily precipitation distribution	mm
p99th	99th percentile of daily precipitation distribution	mm
R10	annual count of days with precipitation > 10 mm	days
R20	annual count of days with precipitation > 20 mm	days
CDD	consequetive dry days when precipitation <1 mm	days
CWD	consequetive wet days when precipitation >1 mm	days
NWD	annual total days when precipitation >1 mm	days

2.4 Evapotranspiration modeling with Penman-Monteith

Evapotranspiration was modeled to determine water balance trends. Water balance was estimated as precipitation minus evapotranspiration. Evapotranspiration λE was determined using the Penman-Monteith approach as recommended by Vilà-Guerau de Arellano (2015) in chapter 9.2.2:

$$\lambda E = \frac{\varrho c_p \frac{(e_s(T)-e)}{r_a} + \Delta \cdot (R_n - G)}{\Delta + \gamma(1 + \frac{r_s}{r_a})} \tag{1}$$

and is calculated from net radiation R_n at the vegetation surface, soil heat flux G, vapor pressure e, saturation vapor pressure e_s, dry air density ϱ, specific heat capacity of air c_p, atmospheric conductance r_a, psychrometric constant γ and stomatal resistance r_s. Net radiation was calculated out of all radiation devices listed in table 2. The soil heat flux was assumed to be 5% of net radiation. Vapor pressure and saturation vapor pressure were calculated from relative humidity and air temperature. The specific heat capacity of air and the psychrometer constant are both constants.
Stomatal resistance r_s was calculated after Vilà-Guerau de Arellano (2015) using the Jarvis scheme (see equation 2.2) and was calculated using the minimum stomatal resistance $r_{s,min}$, the leaf area index LAI, a correction factor f_1 for short wave downwelling radiation S_{in}, a function f_2 depending on soil moisture w from a depth of 10 cm, f_3 as a function of the vapor pressure deficit VPD and f_4 as a function depending on temperature T.

$$r_s = \frac{r_{s,min}}{LAI} f_1(S_{in}) f_2(w_{soil}) f_3(VPD) f_4(T) \tag{2}$$

The corresponding functions are the following:

$$\begin{aligned}
\frac{1}{f_1(S_{in})} &= min\left(1, \frac{0.004 S_{in} + 0.05}{0.81(0.004 S_{in} + 1)}\right) \\
\frac{1}{f_2(w)} &= \frac{w_{soil} - w_{wilt}}{w_{fc} - w_{wilt}} \\
\frac{1}{f_3(VPD)} &= exp(-g_D VPD) \\
\frac{1}{f_4(T)} &= 1.0 - 0.0016(298.0 - T)^2
\end{aligned}$$

where w_{wilt} is the soil moisture at wilting point and w_{fc} the soil moisture at field capacity. The modeled evapotranspiration data was compared to measured Eddy-covariance evapotranspiration data in mm of the Weidenbrunnen site from 2002-2012. The modeled data fit the measured data with an R squared of 0.56 (see figure 35, appendix). Some site-specific constants were adjusted from literature values to ensure a better overlap between modeled and measured data (see table 4). Multiple seasons showed good alignment between both data sets. 1998 was eliminated from the yearly evapotranspiration trend analysis, because measurements only started in late March, therefore influencing annual sums. Leila Schuh (2017) worked in her master thesis on a land surface model customized to the Waldstein site in 2003 and 2004, therefore providing high-quality reference data for this thesis.

2.5 Data processing and gap filling

Daily-, 10 min precipitation data and the variables for the Penman-Monteith model were available for different periods (see figure 2).

Table 4: Site Specific Parameters

Parameter	Literature	Value	Final Value
lower radiation limit RGL	Leila Schuh (2017)	30	30
min stomatal resitance	Leila Schuh (2017)	158	200
max stomatal resitance	Leila Schuh (2017)	2500	5000
LAI	Foken and Lüers (2015)	4.8 (2012)	4.5
soil moisture, field capacity	Leila Schuh (2017)	11.4%	10
soil moisture, wilting point	Leila Schuh (2017)	19.5%	20
g_D	Vilà-Guerau de Arellano (2015)	0.03	0.15
measurement hight	Foken and Lüers (2015)	14.3 m	14.3 m
roughness length	Leila Schuh (2017)	2.0 m	2.5 m

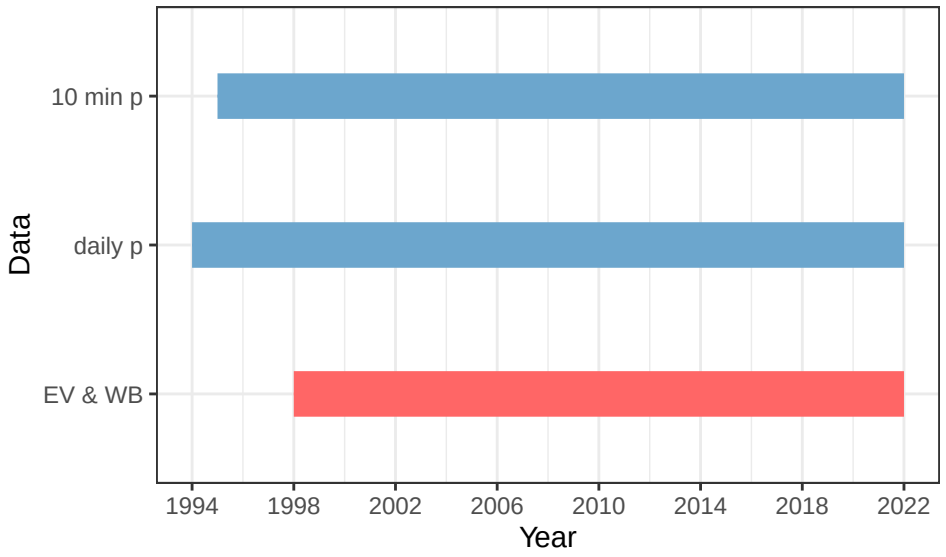

Figure 2: Data availability for 10-minute precipitation data, daily precipitation data, modeled evapotranspiration, and calculated water balance data.

10 min data was not filled because of the high sensitivity for variance. All 10-minute winter measurements from 1995-2003 had to be disregarded, because of a device malfunction in freezing conditions. This limits event-based analysis and 10-minute intensity analysis of precipitation to spring to autumn for this period. Additionally, in 2016, the measurement threshold for precipitation changed from 0.1 mm to 0.01 mm. This resulted in more small-scale precipitation events, with little precipitation sum. This needed to be corrected for data before and after this change to be comparable. From 2016 onwards, precipitation measurements were rounded down to one decimal place, and the second decimal place was added to the next measurement interval. This simulated a measurement threshold of 0.1 mm in the first place.

Daily precipitation data was filled by Johannes Lüers and Wolfgang Babel with data from the Fichtelberg station run by the German Weather Service. The Fichtelberg station is 20 km southward and 110 m lower than the Waldstein site.

For the evapotranspiration model, temperature data was filled with data from the Pflanz-

garten site, sonic temperature data from the Weidenbrunnen site, and the remaining 1.9% with a yearly average. Relative humidity data was filled with Pflanzgarten data, calculated from the Frankenberger Psychrometers, and the remaining 2.6% with a yearly average. For wind speed, the Thies 2D-ultrasonicR3-50 was the reference. Data gaps were filled with cup anemometer data and Pflanzgarten data. The remaining 12.5% were filled with a yearly average. Little data was available for soil moisture because soil moisture measurements started only in 2008. Therefore, 45% of the soil moisture data had to be filled with a yearly average. For air pressure, 3.7% had to be filled with a yearly average. All radiation data was not filled in. This amounted to 11.5% missing data of evapotranspiration, which was filled with a yearly average. Before evapotranspiration data was filled, the model was adjusted to fit the Eddy-covariance data.

The functions for event-based analysis of precipitation and modeling of evapotranspiration were written by Wolfgang Babel and customized in collaboration (see appendix). Kendall's-Tau was used to analyze the significance of precipitation and evapotranspiration trends. Trends were deemed significant if their p-value was below 0.5. The fitted linear models in plots were calculated through linear regressions and are only apparent when a trend was significant. Analysis, modeling, and gap-filling was done in R-4.2.2. All data were visually checked for outliers and corrected.

3 Results

We investigated, how different statistical methods of precipitation analysis explain the overall trend of precipitation and consequently water balance. Firstly, precipitation and water balance trends were determined on a yearly, seasonal, and monthly scale. Afterward, the changes in precipitation characteristics using indices were studied. Lastly, trends inside the precipitation distribution were analyzed through event-based analysis and precipitation intensities. Blue bar plots show measures of precipitation, red bar plots evapotranspiration, and yellow bar plots count days of a parameter.

3.1 Precipitation trends

Precipitation and temperature were measured between 1994 and 2022, and summed up and averaged to monthly, seasonal, and yearly values respectively, to determine underlying trends. Monthly averages of precipitation and temperature were determined to gain a basic understanding of the climate characteristics at the Waldstein site.

For temperature, there was a distinct maximum in summer (July) with 16 $°C$ and a minimum in winter (January) at -2.5 $°C$ of average monthly temperature (figure 3). Temperature experienced little relative variability each month and had a gradual incline towards summer and a decline towards winter over each year. An annual mean temperature of 6.68 $°C$ was detected with an average rise of 0.06 $°C$ per year (figure 24, appendix). This greatly exceeds the rates of temperature rise detected by past studies for this region.

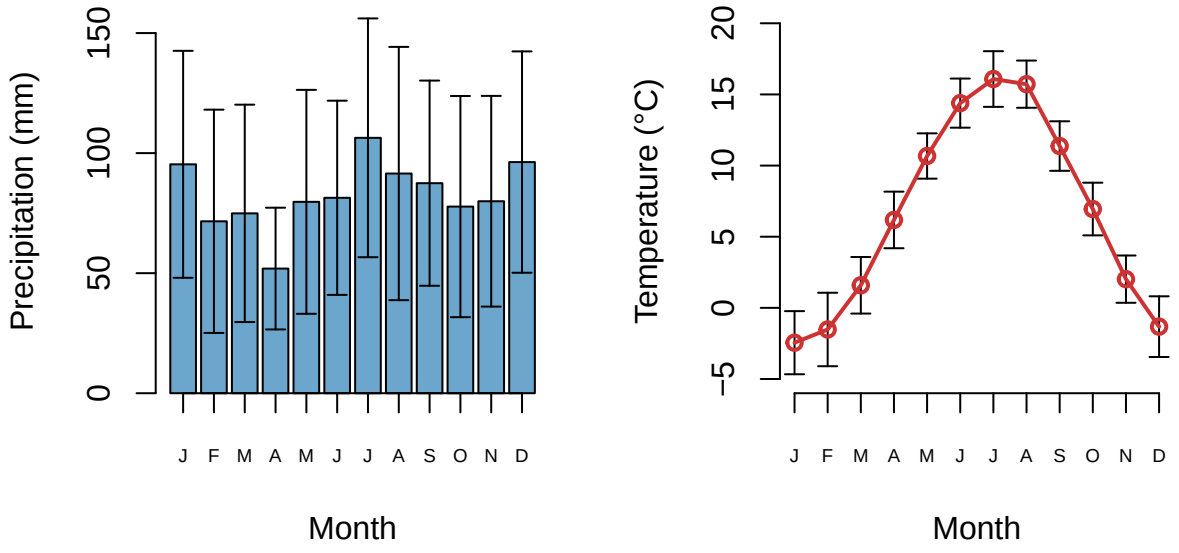

Figure 3: Averages of monthly precipitation (left) and temperature (right) with arrows as standard deviations from 1994 to 2022.

Precipitation at the Waldstein site had two peaks, one in summer and one in winter.

Precipitation was lower in Autumn, but lowest in Spring. Average monthly precipitation reached its primary peak in July with 106 mm and its secondary in January with 96 mm. Average monthly precipitations' smallest monthly mean was measured in April, with 52 mm. In contrast to temperature, monthly precipitation varied greatly, with standard deviations up to 53 mm, or 57 % of the monthly mean, in August.

Annual precipitation experienced a downward facing trend of 9 mm per year, despite significant annual variability (figure 4). However, with the decline in annual precipitation, variability decreased as well. The two wettest and dryest years were within the first half of the observation period. On average, the Waldstein site experienced 994 mm of annual precipitation. Nevertheless, the recorded decreasing trend vanishes when the observation period is limited to 1996-2020. This illustrates that, because of precipitation's high variability, perspective matters when determining trends. Historically dry years like 2018 are represented in the data. Although 2018 does not stand out as much when compared to the years before and after for example 1997 or 2003. The variability of annual precipitation declined over the observation period.

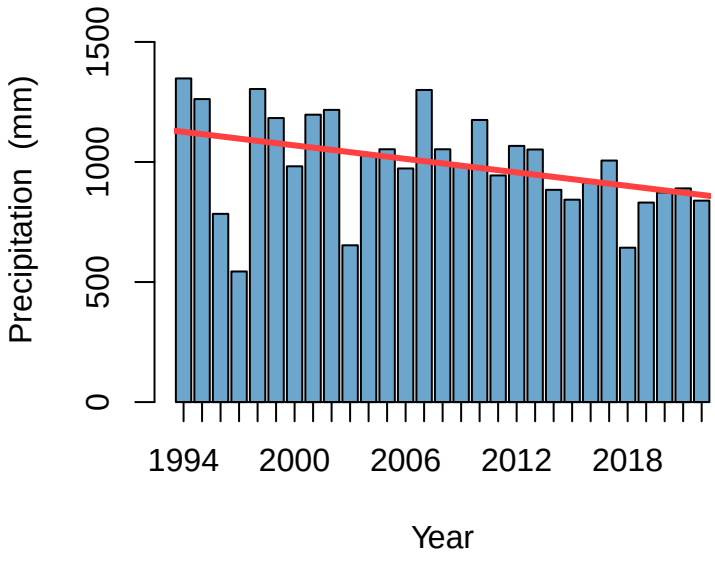

Figure 4: Annual precipitation from 1994 to 2022. (trend: p=0.004, slope m=-9.3 mm/year).

On a seasonal level, summer was the wettest season, and spring was the dryest season with 279 mm and 206 mm on average respectively (figure 5). This correlates well with observations of monthly maximums and minimums in figure 3. However, only summer recorded a significantly decreasing trend. In spring, it only seemed like there was a decrease in precipitation, but statistically, there is no trend. When defined hydrologically, summer only had a nonsignificant decreasing tendency (figure 26, appendix). Hydrological spring and autumn displayed slightly decreasing tendencies, which could not be statistically confirmed. An increase in seasonal precipitation in winter was visually determined, however,

without any statistical significance. All seasons experienced great precipitation variability, with differences in precipitation in autumn of up to 346 mm. Analysis of monthly precipitation has shown that only in July, there is a declining trend in precipitation (figure 25, appendix). No other month showed a statistically significant trend towards more or less precipitation. Visually, however, March had a decreasing tendency, and December and January had an increasing tendency.

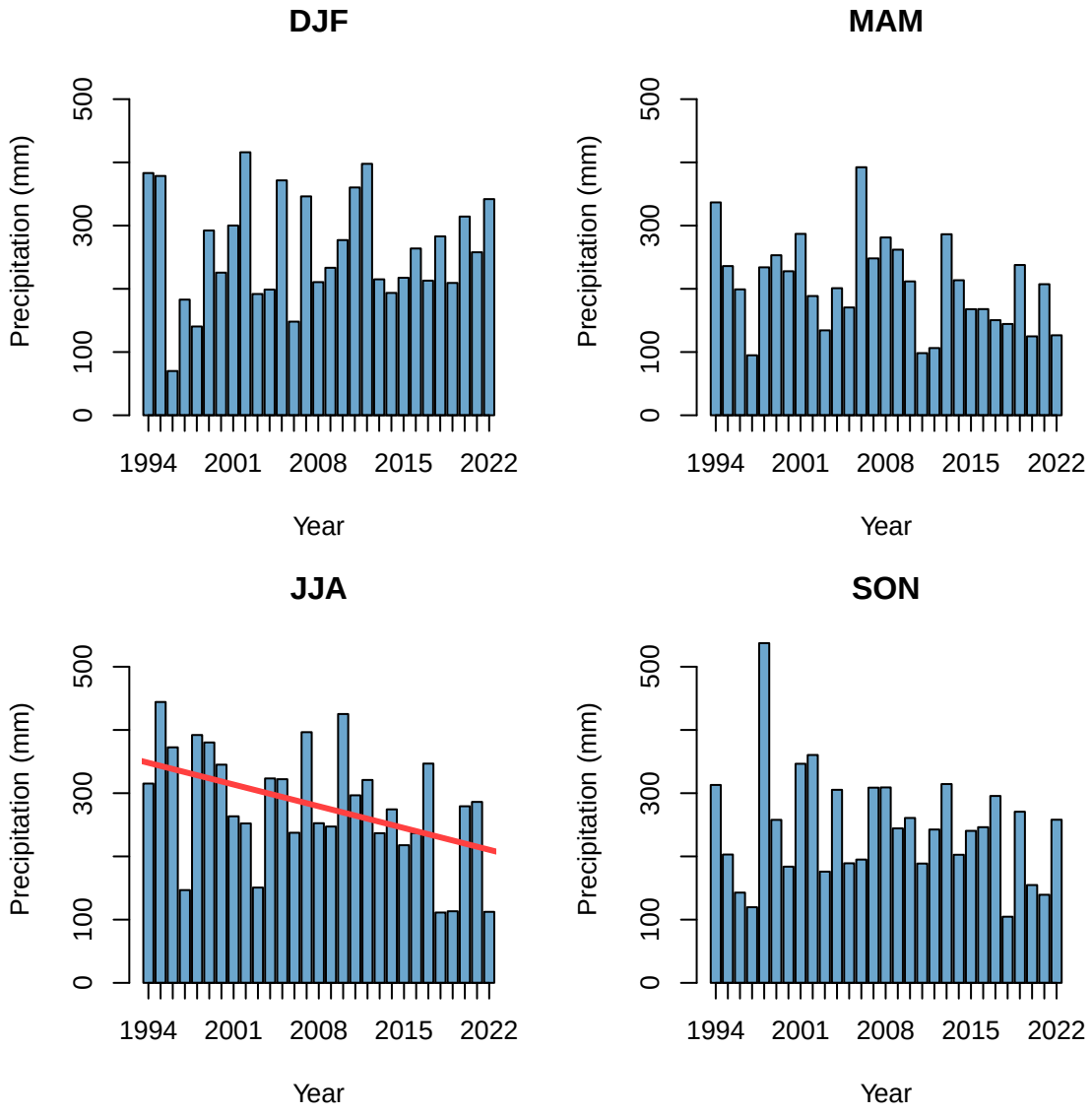

Figure 5: Seasonal precipitation sums from 1994 to 2022. (summer trend: p=0.013, m=-4.9).

In summary, there was a decreasing annual trend in precipitation, which had its base in summer, July. Precipitation trends depend greatly on their observation period, which is not the case for temperature. This dependence is based on the high variability of precipitation.

3.2 Water balance

Evapotranspiration rates were highest in summer and lowest in winter (figure 6). The highest monthly average evapotranspiration rate was in June with 63 mm, and the lowest in January with 1.2 mm. Evapotranspirations yearly development was quite similar to temperatures. Evapotranspiration varied relatively little, resulting in low standard deviations. Water Balance, on the other hand, had its peak in winter in decreased towards summer, where it increased again until winter. Water balance displayed the almost exact opposite trend to evapotranspiration, having its maximum monthly average in December at 95.6 mm, and its primary minimum in April at 18 mm. Between April and August, it was within one standard deviation to have a negative water balance, although on average, no month had a negative water balance. While evapotranspiration varied relatively little, water balance had much higher standard deviations, resulting from precipitations' high variability. Because monthly precipitation displayed a much smaller amplitude in figure 3 than evapotranspiration, the course of water balance over a year is primarily driven by evapotranspiration.

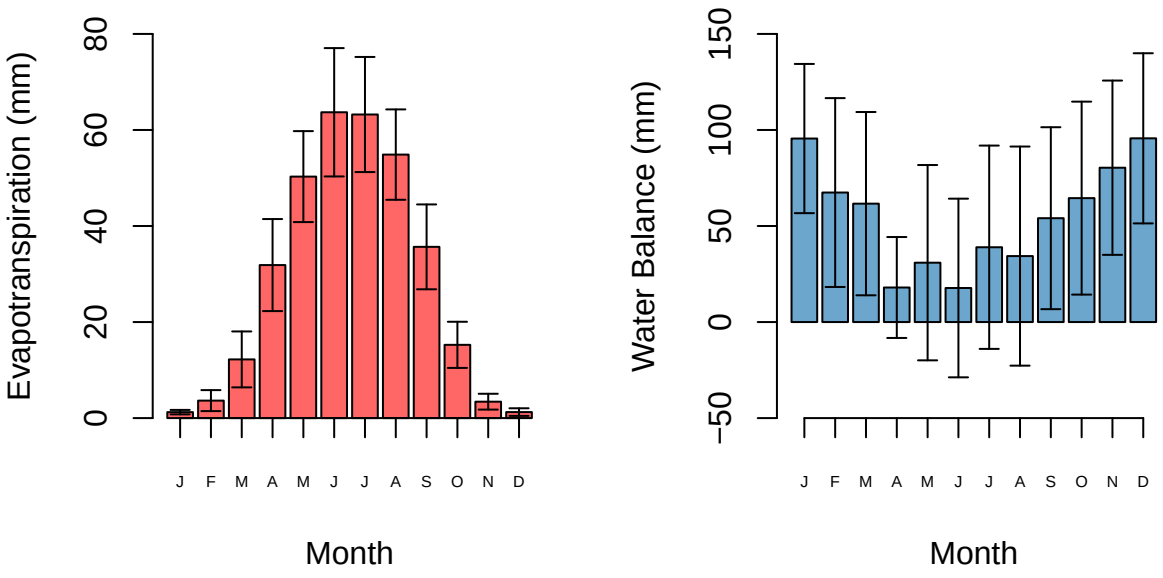

Figure 6: Monthly means of evapotranspiration (left) and water balance (right).

Over the observation period, evapotranspiration showed a significantly decreasing trend (see figure 7). Evapotranspiration had an annual average of 330 mm and varied between 427 mm in 2003 and 247 mm in 2021. Only in 2018, 2020, and 2021, evapotranspiration was below 275 mm a year. As a control, potential evapotranspiration was calculated using Pristley-Taylor, which increased over time. From all parameters that influenced the model of evapotranspiration, soil moisture was the only one that had a decreasing trend, however, a nonsignificant.

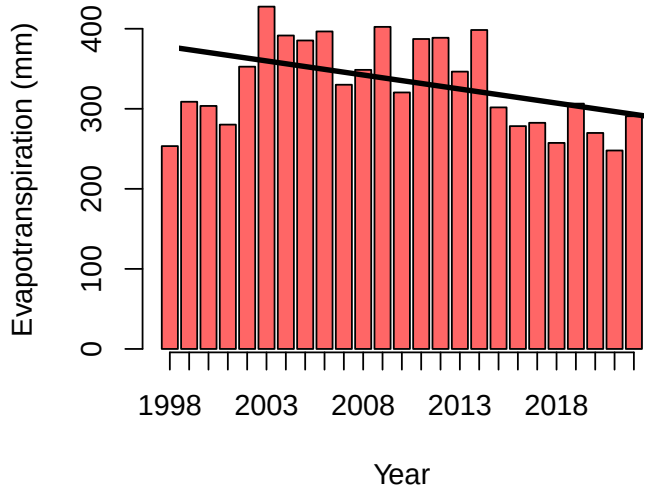

Figure 7: Yearly sum of evapotranspiration. (trend: p=0.01, m=-3.51)

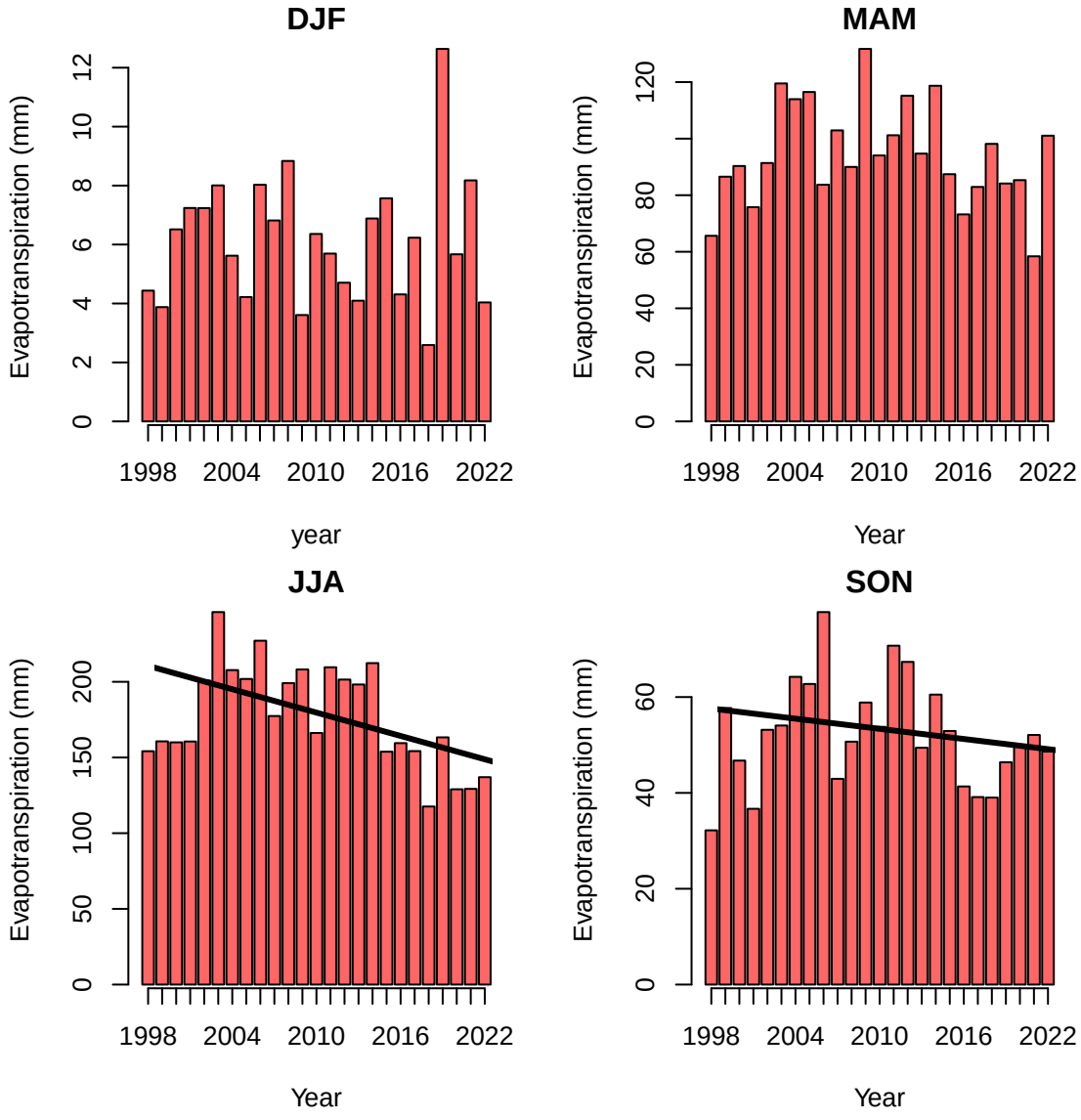

Figure 8: Seasonal evapotranspiration. (trend summer: p=0.057, m=-2.5 , trend autumn: p=0.050, m=-0.35)

On a seasonal scale, evapotranspiration decreased extensively in summer, and in autumn to a smaller degree (figure 8). Winter and spring were not affected by any trend. Both trends were also visible when seasons were defined hydrologically. However, they were more similar in slope (figure 27, appendix). Visually, a small increase in evapotranspiration was detected in hydrological spring. On a monthly scale, evapotranspiration decreased over the observation period from May to August (figure 28, appendix). Summer is also the season, in which precipitation decreased most significantly. Additionally, nonsignificant decreasing evapotranspiration tendencies were found in September.

Water balance showed a significantly decreasing trend over the years and averaged at 665 mm (figure 9), indicating that precipitation decreased at a higher rate than evapotranspiration. Interestingly, the lowest water balance was recorded in 2002 with 225 mm, due to high evapotranspiration and low precipitation. Water balance reached its peak in 2007 at 1050 mm.

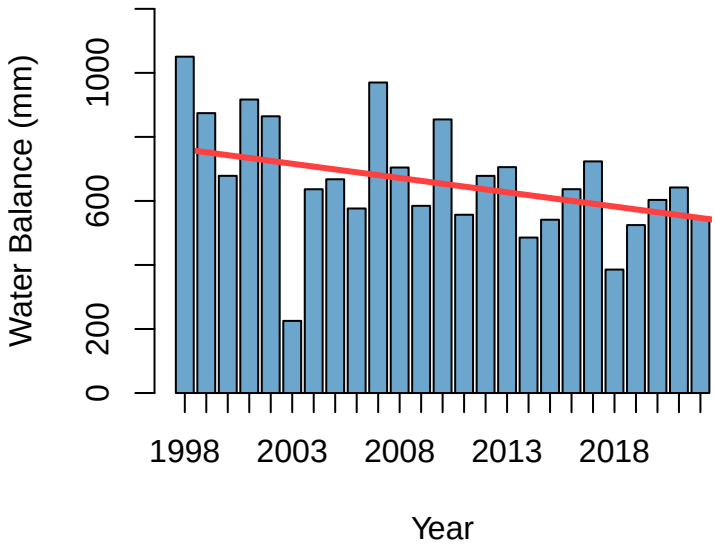

Figure 9: Yearly water balance. (trend: p=0.01, m=-8.9)

On a seasonal level, there was a decreasing trend for water balance in spring, and a visually decreasing tendency for summer and August (figure 10). While water balance declined fastest in spring, summer recorded more frequently negative values, especially in the last decade. Winter showed no trend. Regarding hydrological seasons, no season had a significant water balance trend (figure 29, appendix). Although, summer and Autumn looked like they had decreasing trends. On a monthly scale, only July experienced significantly less water balance over the years (figure 30, appendix).

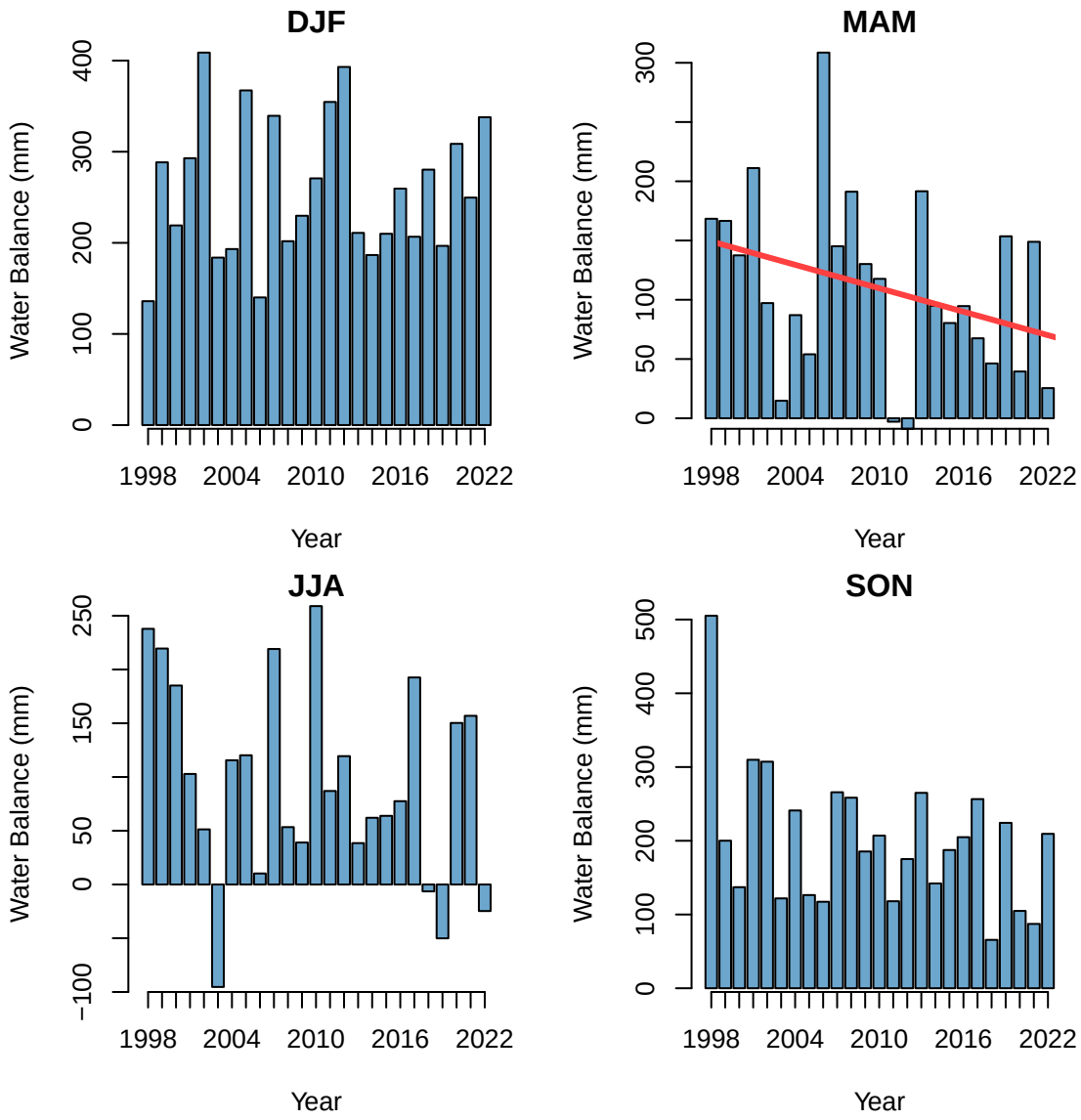

Figure 10: Seasonal water balance. (trend MAM: p=0.04, m=-3.3)

In conclusion, water balance declined, even though evapotranspiration decreased over the years, especially in the summer months. Water Balance was mainly affected in spring and July. Overall, the decrease in precipitation outweighed the decline in evapotranspiration.

3.3 Indices of precipitation

To determine the characteristics of precipitation at the Waldstein site and their tendency, precipitation indices were calculated. They give insight into the extremes and the distribution of precipitation. All indices were calculated out of daily sums of precipitation.

Firstly, the number of wet days NWD per year, the maximum number of consecutive wet days CWD, and maximum number of consecutive dry days CDD per year were in-

vestigated. These indices give insight into the yearly distribution of precipitation. The Waldstein site experienced on average 140 NWD (figure 11). NWD was relatively stable, but the data showed that NWD declines by almost 1 per year on average. When limiting the observation period to 1996-2019, the trend disappeared. Additional analysis presented, that NWD correlated with annual precipitation (figure 12), meaning that average daily precipitation intensity was stable.

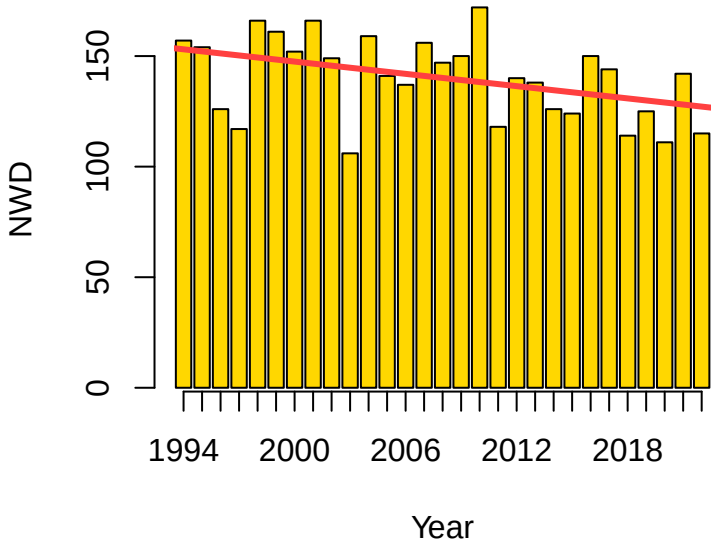

Figure 11: Number of wet days NWD with precipitation above 1 mm per day. (trend: p=0.007, m=-0.9).

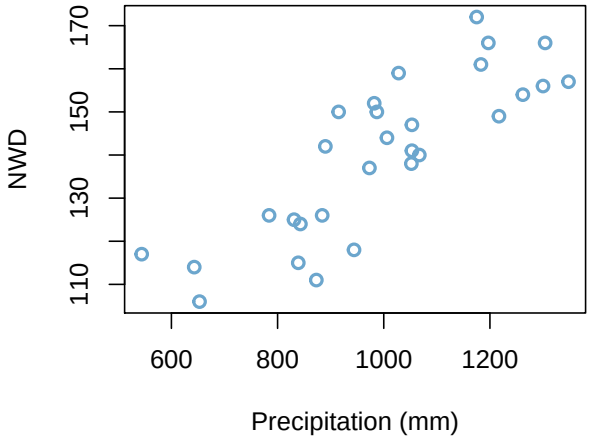

Figure 12: Number of wet days per year against annual precipitation. (correlation p=0.000).

CWD and CDD averaged at 9.6 and 19 days (see figure 13). There was no trend for both, furthermore, they did not share a similar pattern over the years. Both experienced decent variability.

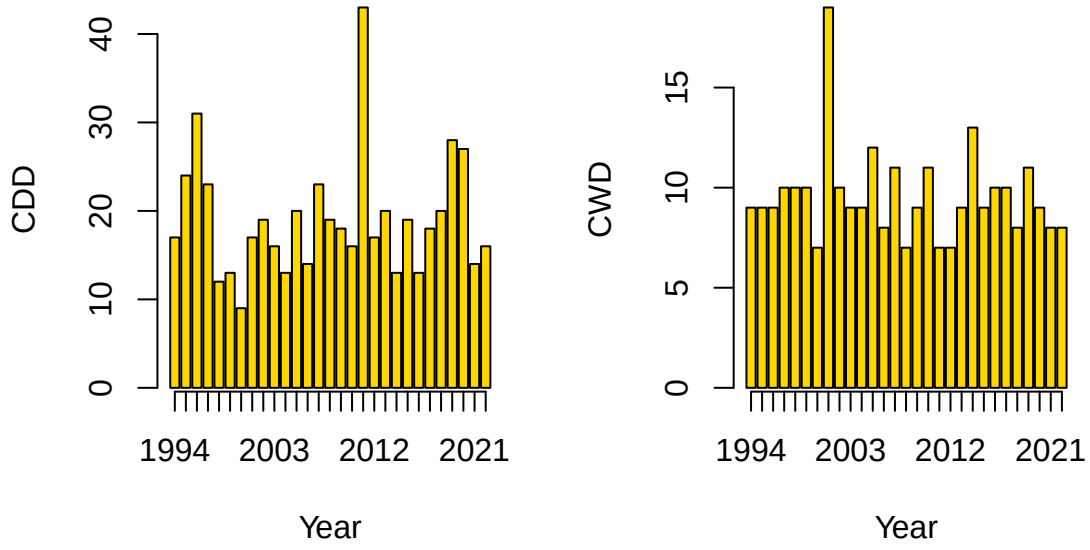

Figure 13: Consecutive dry days CDD (left) and consecutive wet days CWD (right).

Two indices indicating the extremes of precipitation are maximum one day precipitation (RX1day) and maximum 5-day precipitation (RX5day). While RX1day decreased over the years quite significantly, RX5day was stable (figure 14). The mean RX1day was 45 mm and the mean RX5day was 65 mm. RX1day peaked at 79 mm in 1996 and RX5day at 111 mm in 1998. Rx5day showed greater variability than RX1day. RXday5 was not many times higher than RXday1 considering the 5 times longer observation period. Visually, there is no indication that both indices were connected.

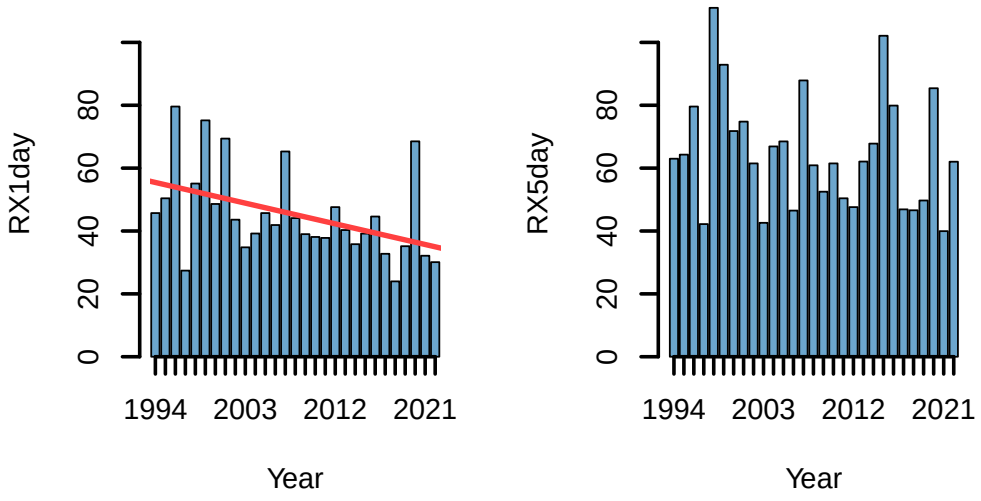

Figure 14: Maximum precipitation fallen over one day RX1day (left) and 5 days RX5day (right) per year. (trend RX1day: p=0.001, m=-0.73).

Another indication for precipitation extremes is precipitation fallen above the 95th percentile (R95p), and 99th percentile (R99p) (figure 15). Both showed significant trends towards less precipitation above their respective thresholds and fluctuated around a mean

of 211 mm for R95p and 77 mm for R99p. Visually, they seemed to be linked, sharing most maximums and minimums besides their general trajectory. Looking only at the development of the 95th and 99th percentile exclusively, only the 99th percentile decreased statistically significantly (figure 31, appendix).

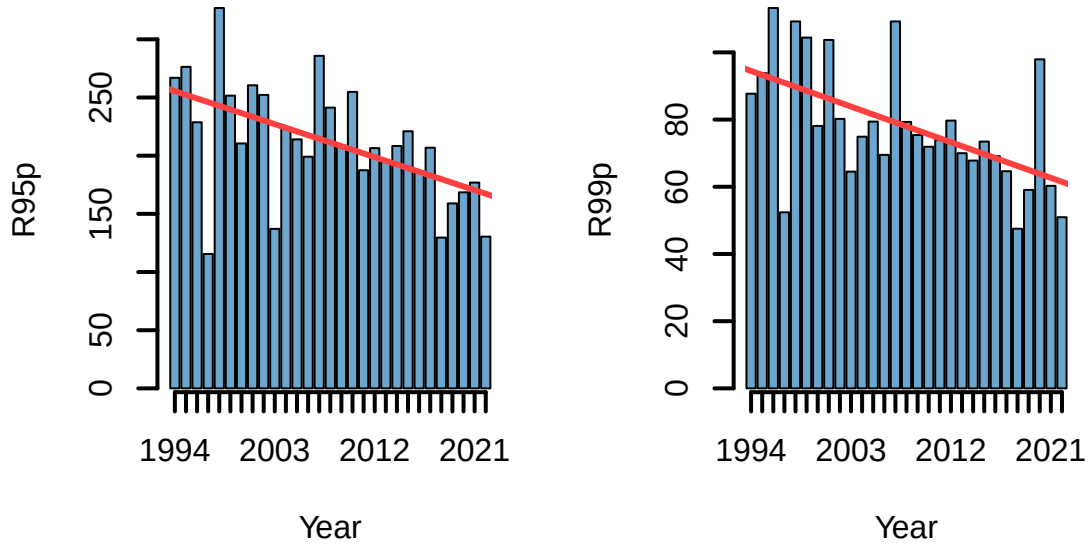

Figure 15: Precipitation fallen above the 95th percentile R95p (left) and 99th percentile R99p (right). (trend R95p: p=0.0002, m=-3.1; trend R99p: p=0.0001, m=-1.1).

A different approach to identifying extreme precipitation is to count the days with precipitation above a certain threshold. R10 and R20 represent heavy and very heavy precipitation days, which count precipitation above 10 mm and 20 mm a day, respectively. The Waldstein site experienced on average 29 days R10 and 8 days R20 (figure 16). R10 and R20 decreased between 1994 and 2022, with relatively high variability. But both trends fade when excluding 1994 from the analysis, which had particularly high R10 and R20.

In summary, NWD and multiple indices describing extreme precipitation decreased. The Waldstein site experienced less precipitation overall, and the one it received, seemed to be more modest.

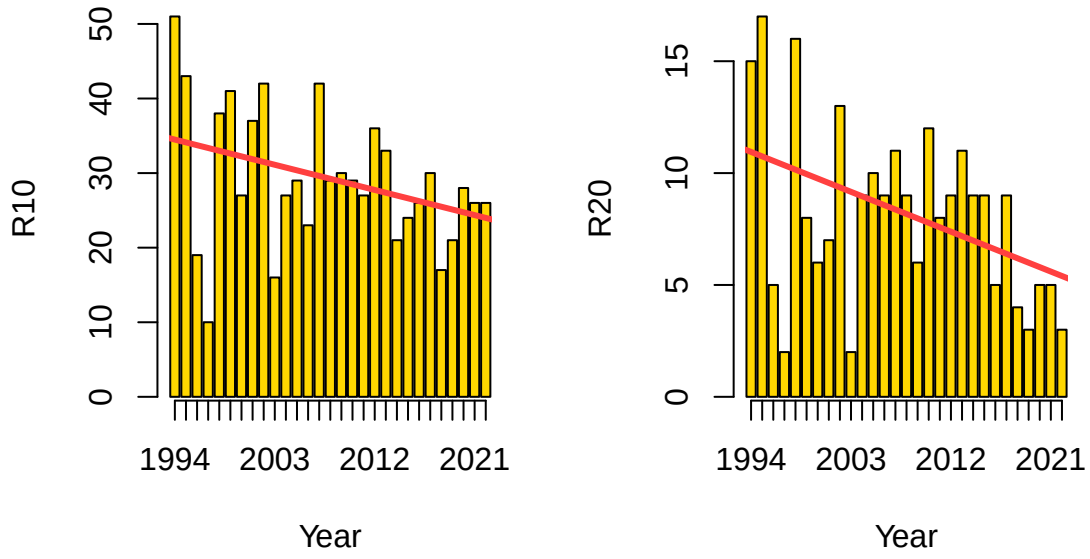

Figure 16: Number of days with precipitation greater than 10 mm per year R10 (left) and 20 mm per year R20 (right). (trend R10: p=0.050 , m=-0.37. trend R20: p= 0.040 , m=-0.19)

3.4 Precipitation events and intensities

For this section, 10-minute data was analyzed to get insight into a more accurate representation of precipitation intensity. Precipitation intensity was defined as measured precipitation in 10 minutes. Precipitation event intensity, on the other hand, describes the mean or maximum intensity of a precipitation event. A precipitation event had precipitation for more than 10 minutes or more than 0.1 mm event precipitation sum. As all winter data was deleted from 1994-2003, the observation period was limited to 2004-2022 for the trend analysis.

The mean monthly precipitation intensity had its maximum in summer July and declined towards winter (figure 17). This pattern was similar to temperature and evapotranspiration. With rising intensity throughout the year, the average variability increased as well. The minimum average intensity was in January at 0.17 mm and the maximum in July at 0.41 mm. For yearly mean precipitation intensity, visually, there was a decreasing trend. However, there was no significant trend from 2004-2022. Winter precipitation, which was deleted from 1998-2003 (see chapter 2.5), had less intensity on average, therefore, increasing the mean before 2003. On a monthly scale, only April showed an increasing trend, all others showed just variability (figure 32, appendix).
Mean and maximum precipitation event intensity decreased quite significantly over the years (2004-2022) (figure 18). The average mean event intensity was 0.23 mm and the maximum event intensity was 0.44 mm. A more in-depth analysis of maximum event intensity showed, that its distribution narrowed over time towards lower intensities (figure 33, appendix). As a measure of extreme precipitation, the 95th percentile of the maxi-

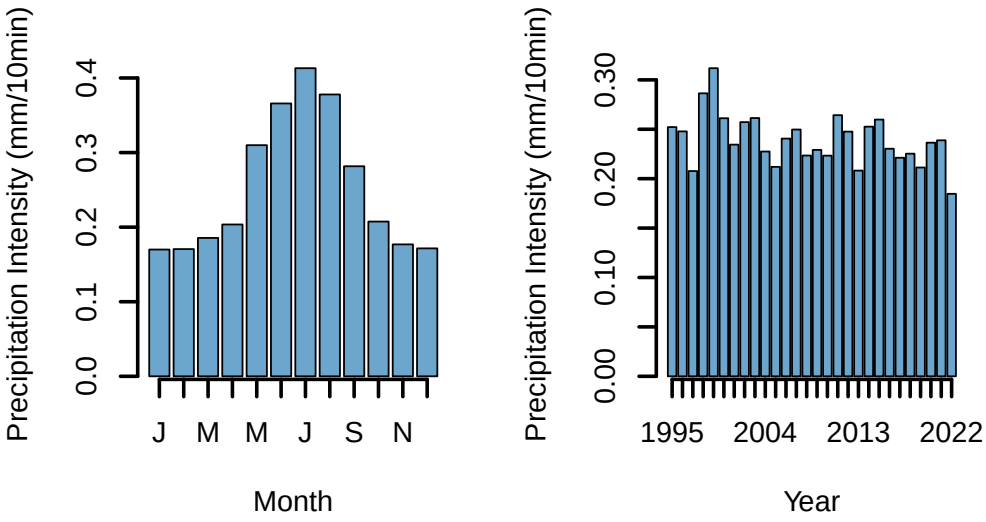

Figure 17: Average monthly precipitation intensity (left). Yearly mean precipitation intensity (right).

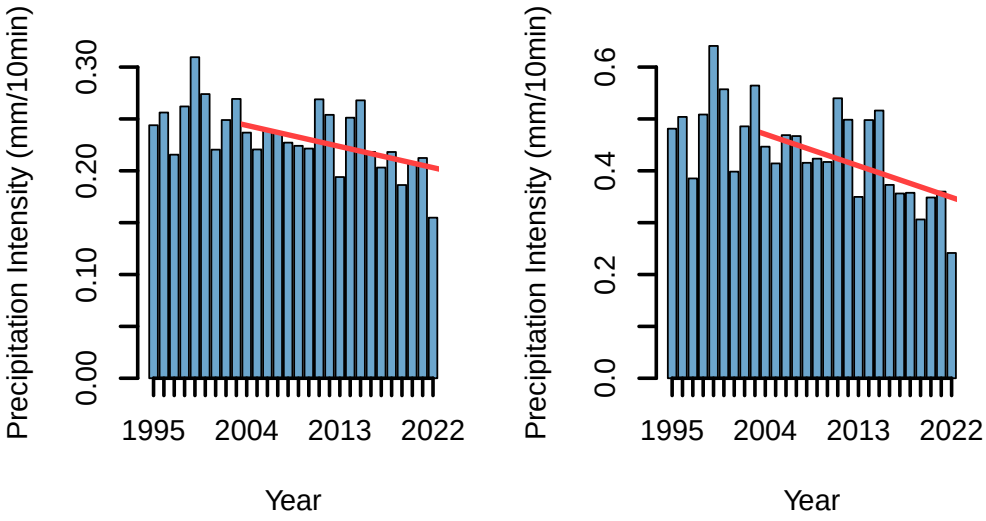

Figure 18: Mean event intensity (left) and maximum event intensity (right). (trend left: p=0.010, m=-0.002. trend right: p=0.015, m=-0.006).

mum event intensity was analyzed. The 95th percentile of the maximum event intensity decreased significantly over the observation period (figure 19). This value had its two lowest points in the last 4 years. Comparing that with the number of events per year, there was an increasing trend. This increase in the number of events, however, was not statistically significant, when limiting the observation period to 2004-2022. The number of events fluctuated around 543 events per year on average and had its peak in 2017 with 777 events. No subgroup of events showed any trend when divided into their respective precipitation sums (figure 34, appendix).

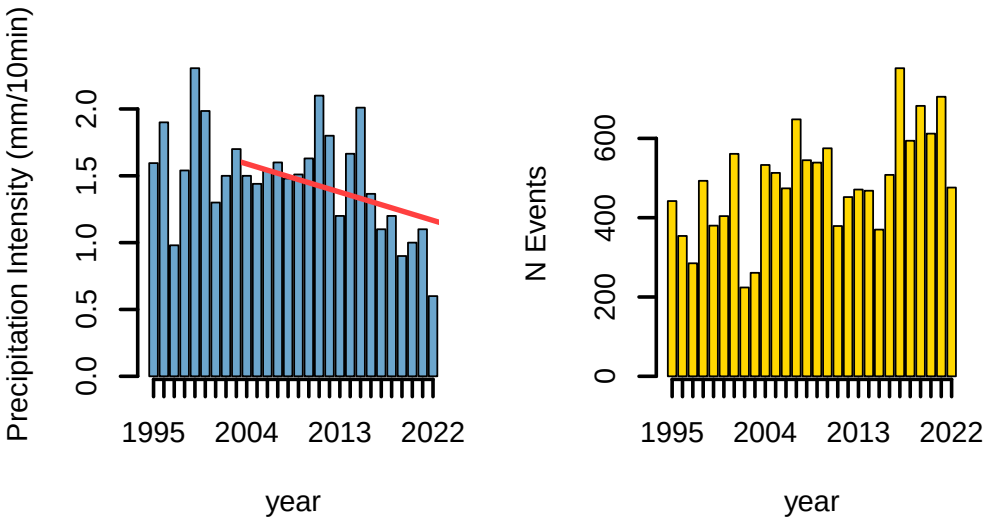

Figure 19: Yearly 95th percentile of maximum event intensity (left). (trend: p=0.008, m=-0.02). Number of events per year (right). (no trend for 2004-2022)

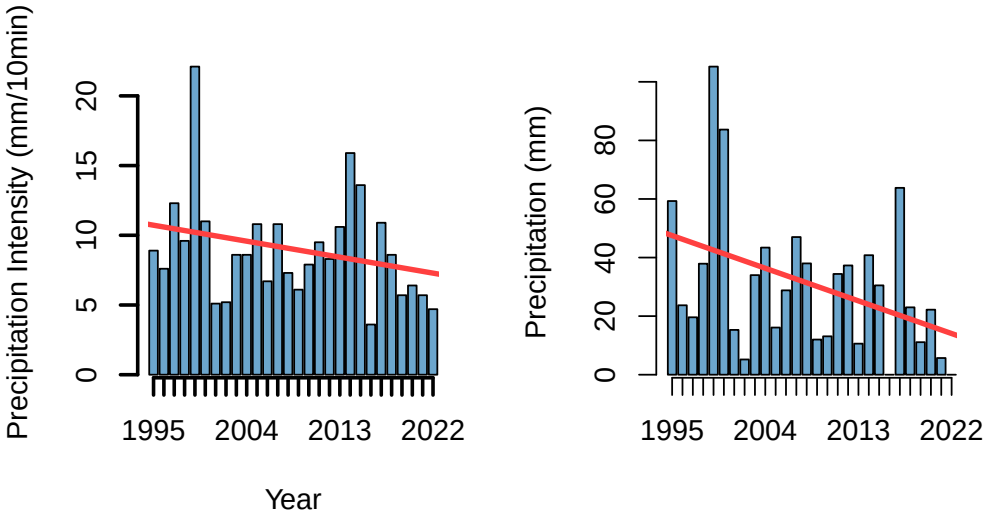

Figure 20: Maximum 10-minute precipitation intensity per year (left). (Trend: p=0.03, m=-0.12). Annual precipitation fallen above the threshold of 5mm/10min (right). (Trend: p=0.025, m=-1.2).

The most extreme precipitation intensities were investigated using the maximum intensity for each year (figure 20). A significantly decreasing trend for the yearly maximum intensity was detected, despite great variability. As precipitation reached the highest intensities in summer, all the years were included in this analysis. Additionally, precipitation fallen above a threshold of 5 mm per 10-minute interval was determined. This value decreased as well. In particular, the last 4 years had very little precipitation above the 5 mm intensity threshold. In summary, mean annual precipitation intensity did not decrease over the years. However, there were decreasing trends for maximum and mean event intensity. All investigated measures of extreme precipitation intensity decreased. The number of events was highly variable but had no underlying trend.

4 Discussion

4.1 Why did precipitation and water balance decrease?

One of the main goals of this thesis was to determine, whether annual precipitation had an underlying trend. We hypothesized, that precipitation will see a seasonal shift, that consequently declines water availability for vegetation.
The data has shown, that annual precipitation has decreased over the observation period. Additionally, spring precipitation decreased non-significantly and summer precipitation significantly, which was mainly driven by significantly decreasing precipitation in July. This trend was already observed by Foken and Lüers (2015). This study is the first to document decreasing annual precipitation in the Fichtelgebirge. Previous research by Lüers et al. (2017) reported stable annual precipitation and even suggested that there is a nonsignificant trend towards more annual precipitation in the Fichtelgebirge.
A possible explanation for the annual decrease in precipitation might be that the number of rainy days decreased, which correlates considerably with annual precipitation. The observed decrease in summer precipitation could be attributed to a shift in weather system dynamics, that are influenced by a global rise in temperature. It is possible, that over the observation period, there has been a continuous increase in the occurrence of stable high-pressure systems. Additionally, the occurrence of convective precipitation could have decreased, which could influence precipitation sums negatively. This is an important issue for future research. A note of caution is due here since this shift could influence local precipitation patterns, which could be compensated by nearby catchment areas. The complex topography of the Waldstein site enables only to a certain degree to scale the observations on the larger area of northern Bavaria. The observed trends often only hold their significance in certain observation periods. Therefore, the made conclusions must be tested regularly. Furthermore, the decline in precipitation could be rooted in increased demand for water vapor to reach saturation with rising temperatures and thus precipitation.
In summary, the findings suggest that the in the past declining spring precipitation has stabilized. However, there will be less precipitation in summer in the future, with fewer rainy days and a diminished supply of water to vegetation as annual precipitation further declines.

For water balance, we hypothesized that there would be a decreasing trend, due to a seasonal shift in precipitation. Indeed, the annual water balance decreased. There was no shift in precipitation, only a decrease in spring and summer precipitation, and consequently in annual precipitation, as no other season compensated for missing spring and summer precipitation. Water balance decreased even though annual evapotranspiration decreased as well, with May to August showing decreasing trends. Therefore, there was

a steeper decline in precipitation than in evapotranspiration.
These findings broadly support the work by Lüers et al. (2017), who found decreasing water balance trends as well. However, they attributed this trend to a seasonal shift in precipitation, with decreases especially in spring, as they observed stable to slightly increasing annual precipitation. In conclusion, there were decreasing water balance trends for spring and summer. It can therefore be assumed that water availability decreases annually, but especially during the growing season which could result in drought stress for vegetation. This could leave vegetation more vulnerable to vermin and diminish populations that rely on water closer to the soil surface, as the water table lowers. It could be argued, that, because extreme precipitation declined and runoff was not measured, water balance was overestimated in the early parts of our observation period. Therefore, the declining trend in water balance could be weaker. Although, groundwater levels are rarely influenced by runoff in the Lehstenbach catchment (Lischeid et al., 2017).
In summary, the results indicate an ongoing decrease in water balance, due to a decline in annual precipitation, which will negatively impact water availability for present ecosystems. However, the findings might not represent trends for all of northern Bavaria, as this study contradicts local research, which could be based on the complex topography of the discussed region.

4.2 Why did extreme precipitation reduce?

We hypothesized that extreme precipitation would rise, as is the case for Europe (Sun et al., 2021) and the World on average (Dunn et al., 2020). Past studies reported no increase in extreme precipitation at this site (Foken, 2003), and hypothesized that it is likely that extreme precipitation will increase in the future (Foken and Lüers, 2013).
Surprisingly, extreme precipitation declined in frequency, amplitude, and volume over the observation period. This trend was visible both in precipitation indices, like R10, R99p, and RX1day, and sub-daily analysis, for example, the 95th percentile of precipitation intensity or precipitation fallen with an intensity above 5 mm per 10 min. However, precipitation intensity increased in April, which is consistent with observations made by Lüers et al. (2017). Observation of declining extreme precipitation percentiles could be explained by the overall shift towards more low-intensity precipitation and a higher number of precipitation events. This shift in precipitation distribution affects measures of extreme precipitation, which display their share in the annual precipitation distribution, e.g. R95p. However, the volume-based indicators of extreme precipitation likely declined due to the decrease in spring and summer precipitation. With similar seasonal distributions of precipitation in those seasons, there would be less volume of extreme precipitation as seasonal precipitation decreases. Again, this volumetric change of extreme precipitation could be attributed to a change in the weather system distribution. Alternatively, weather fronts could have changed on average to more divided smaller cloud

segments, if there is no change in the distribution of weather systems. This would result from a rise in temperature, but constant water vapor and would explain the increase in several precipitation events. To develop a full picture of extreme precipitation trends in the Fichtelgebirge, additional studies will be needed, that investigate the weather system distribution and the ratio between convective and advective precipitation over the observation period. This would give insight into the effects of global warming on large-scale atmospheric circulations and their local impact. An implication of the results is the possibility, that there will be gradually less extreme precipitation at the Waldstein site, with precipitation being more evenly distributed. This could, to some degree, counterbalance the decline in precipitation, as less precipitation is lost to runoff. Because this is the first study to detect a statistical decrease in extreme precipitation, contradicting expectations from local experts, our findings should be validated regularly.

A comparison with precipitation data from the Botanischer Garten in Bayreuth showed that the decline in extreme precipitation was not so clear for nearby sites. Indices like R10 and R20 showed decreasing trends (see figure 36, appendix), but others like R95p and R99p were constant (see figure 21). Overall, all decreasing measures of extreme precipitation at the Botanischer Garten site declined from a relatively high level. Additionally, all measures of extreme precipitation from 10-minute data and event statistics showed no trend. Concluding, that the observed decrease in extreme precipitation is possibly site specific to the Fichtelgebirge, due to its topography or only of significance in certain observation periods.

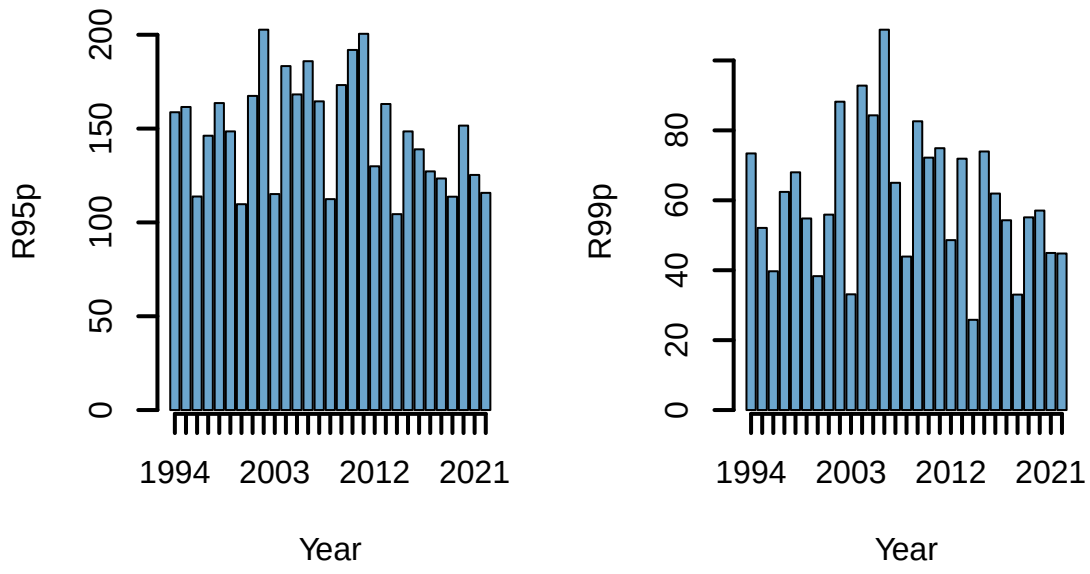

Figure 21: Bayreuth: Precipitation fallen above the 95th perventile (left) and above the 99th percentile (right).

4.3 Is sub daily analysis of extreme precipitation necessary?

Additionally to precipitation indices, extreme precipitation was analyzed using sub-daily data and event statistics. We hypothesized that sub-daily analysis of precipitation is crucial for a more precise understanding of extreme precipitation characteristics and trends. The results show, that sub-daily and daily analyses agree on a decline in extreme precipitation. While indices only gave insight into the volumetric distribution, sub-daily data displays the decline in precipitation intensity more clearly. The event analysis proved to be insightful, as the number of events and the number of wet days had contradicting trends. Consequently, sub-daily analysis of precipitation was useful to better understand extreme precipitation and precipitation. However, most of the conclusions about extreme precipitation would still hold, if only precipitation indices would have been investigated. Applying event and sub-daily precipitation analysis is probably more effective when analyzing smaller timescales or singular precipitation events in more detail. Many details are hidden in the averaging process. However, this could be characteristic of the measurement site. For other sites, sub-daily analysis could paint a completely different picture of extreme precipitation. When applying this method to precipitation data from Bayreuth, multiple indices indicated a decrease in extreme precipitation, however, sub-daily analysis showed that this was not the case (e.g. the maximum precipitation intensity and precipitation fallen with an intensity of greater than 5 mm / 10 min, see figure 37 and 39, appendix). For Bayreuth, sub-daily analysis contradicts precipitation indices. The effectiveness of sub-daily analysis depends on the site-specific precipitation characteristics.
In conclusion, sub-daily analysis of extreme precipitation was not necessary to determine extreme precipitation trends. The quality of the sub-daily precipitation analysis was reduced, due to a shorter observation period starting in 2004 and a change of measurement intervals from 2016 onwards, which could have influenced the detection of events and intensities from there on. Subdaily analysis did not add substantially to the extreme precipitation analysis using indices. But it gave insight into how precipitation events happen, and a clearer picture of precipitation intensity, which is vital to estimate runoff and flooding.

4.4 Did the Waldstein climate dry over time?

We expected the climate of the Waldstein site to dry up, due to intensification of precipitation and a seasonal shift in precipitation. The results indicate a gradual lowering of the water table, through a decrease in water balance. However, precipitation did not intensify, which would have meant more runoff and less groundwater renewal. There was a seasonal decrease in water balance in spring, and in July, which is consistent with observations by Foken (2003). Stable maximum consecutive wet and dry days imply, that the Waldstein does not face a significantly higher drought potential. This finding is consistent with that of Franziska Schwab (2021), who discovered that in the extremely dry years of

2018 and 2019, vegetation recovered quickly after long periods of no rain. In summary, it is evident that the Waldsteins climate dries up gradually as the water table decreases, however, no extreme vegetational stress because of a significant increase in drought potential could be observed so far. Because precipitation in mountainous regions is highly variable, it is hard to generalize the observations to the larger region of northern Bavaria. A quick look into precipitation data measured in Bayreuth, showed that surrounding regions experience a greater increase in drought risk, as the number of consecutive dry days increased significantly (see figure 22). As it is for the Waldstein the case, the number of wet days declined in Bayreuth, and the number of events increased (see figure 38 and 39 in the appendix respectively). The potential for droughts in the Fichtelgebirge should be monitored regularly as it has a high capacity to impact present ecosystems.

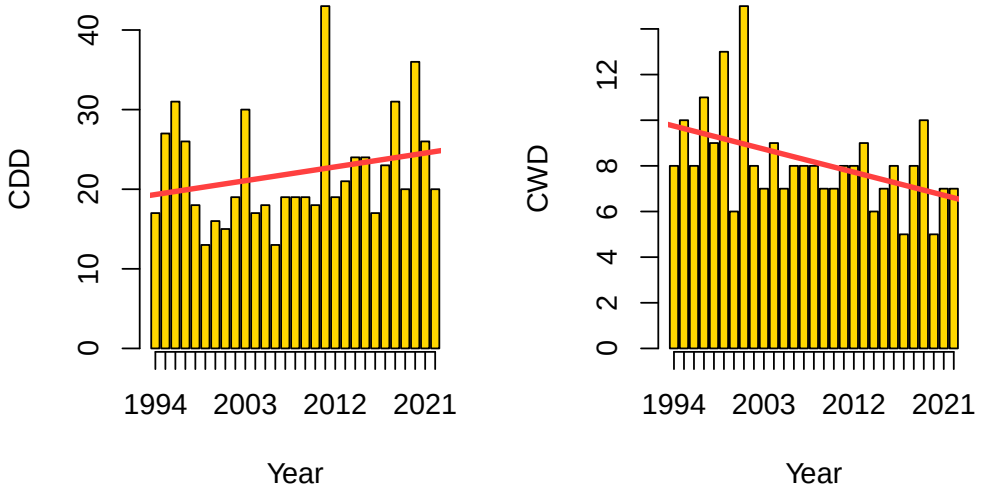

Figure 22: Bayreuth: Number of consecutive wet days (left) and number of consecutive dry days (right) with significant trends.

4.5 Why did evapotranspiration decline?

Evapotranspiration declined against expectations, mainly in summer and spring. On the other hand, potential evapotranspiration rates increased over the observation period. The observed decreasing evapotranspiration trend does not contradict Lüers et al. (2017), who found significantly increasing evapotranspiration rates because evapotranspiration rates also increased in their observation period. In theory, global average evapotranspiration rates rise with temperature, because of the atmosphere's ability to hold more water vapor, consequently increasing the vapor pressure deficit Trenberth et al. (2003).
Of all factors, which could enhance evapotranspiration, only soil moisture had decreased. Although, likely only due to the fact, that soil moisture measurements started in 2008 and had to be gap filled with an annual average before that, eliminating all outliers. This dependence was investigated by filling all soil moisture measurements with an annual

average. Evapotranspiration still decreased, but not significantly. Therefore, soil moisture was not the main cause of a decline in evapotranspiration. Consequently, decreasing evapotranspiration can only be explained by the interaction between its factors.
Firstly, a rising vapor pressure deficit could increase stomatal resistance, lowering evapotranspiration. This is supported by the data, as evapotranspiration in high net radiation conditions generally declined when VPD rose above 15 hPa (see figure 23 left). Again, a change in weather system distribution could cause a rise in the appearance of high VPD and radiation conditions, which have low evapotranspiration rates as stomatal resistance is high.

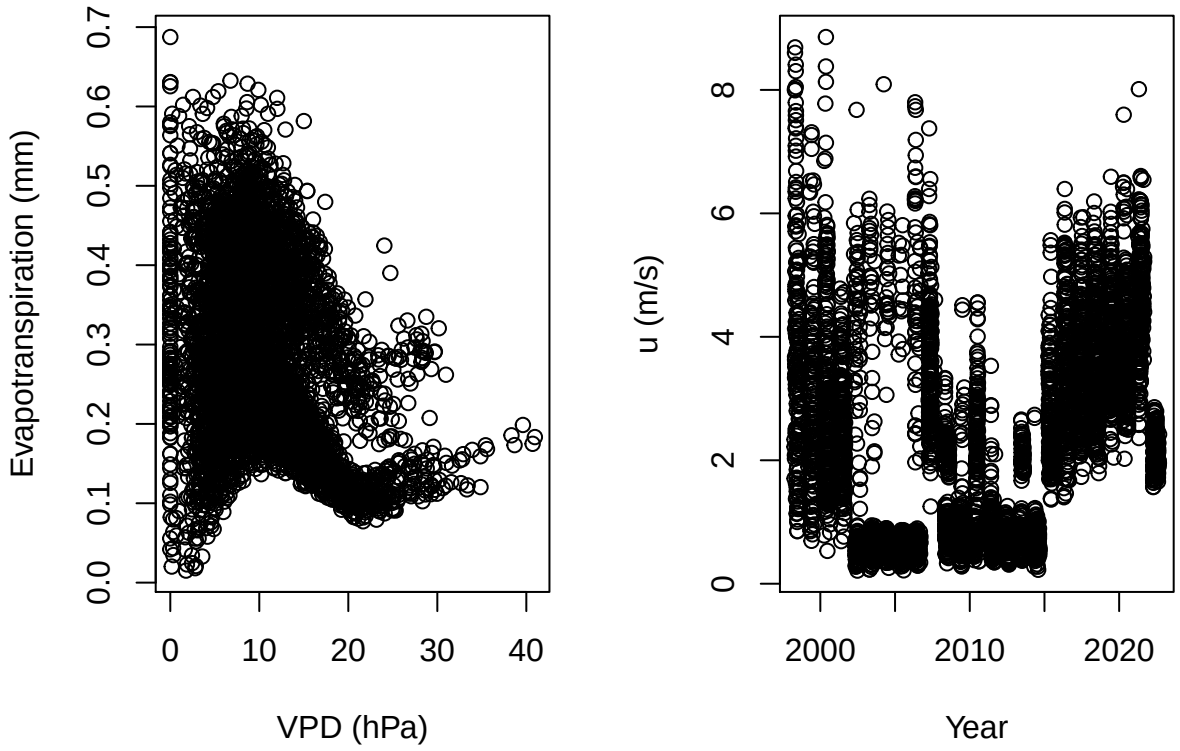

Figure 23: Left: Relation between vapor pressure deficit VPD and evapotranspiration according to Penman-Monteith, when measurements of net radiation were above 600 W/m^{-2}. Right: Measurements of wind speeds u per year when measurements of net radiation were above 600 W/m^{-2}.

Another possible explanation may be, that the decrease in evapotranspiration shares the reasons for declining summer precipitation. A subsequent shift towards more frequent high-pressure systems would lead to longer periods of slower wind speeds. Despite high temperatures, low turbulent mixing would decrease evapotranspiration. This, however, is not supported by the data. When comparing to annual evapotranspiration, wind speeds were lower when net radiation was above 600 W/m^{-2} and evapotranspiration rates were high (see figure 23 right). Consequently, wind speed was not the decisive variable that led to the declining evapotranspiration trend.
These findings might be somewhat limited by the used evapotranspiration model, which

only achieved an R^2 of 0.56 when compared with measured eddy covariance data. In overall trajectory and extent, they are consistent. Additionally, evapotranspiration rates at night tend to be underestimated, which could result in overall slightly underestimated evapotranspiration sums.
In conclusion, evapotranspiration declined most likely, because of the limitation of stomatal conductance by the vapor pressure deficit. A continuous decline in evapotranspiration could lessen the impact of declining precipitation on a lowering water table but also influence the growth rates of the spruce forest.

4.6 Do we face a rapid temperature increase?

Temperature increased with 0.6 K per decade which is almost double what Foken and Lüers (2015) (0.36 K) detected for the larger region of Upper Franconia and significantly larger than what Lüers et al. (2017) (0.4 K) observed for the Waldstein site. The Botanischer Garten site in Bayreuth observed an average increase of 0.5 K over the same observation period.
The temperature rise seems to speed up. Although, in this case, this could be again the result of the observation period, meaning that the slope of this trend fluctuates and depends on the start and end points. However, if this is the beginning of an incline in temperature, this could have severe impacts on ecosystems which already have to cope with a rise in heat stress. This acceleration is being observed globally and is consistent with model evaluations by Collins et al. (2013). Nonetheless, they advocate that the future rise of global temperature depends on future greenhouse gas emissions, and therefore, are hard to predict as those depend on future policies to mitigate climate change.

5 Conclusion

This thesis aimed to determine precipitation and water balance trends, and evaluate extreme precipitation using precipitation indices and sub-daily precipitation analysis between 1994 and 2022 in the Fichtelgebirge.

Annual precipitation declined, which was driven by a decrease in precipitation in summer and spring. The precipitation distribution shifted towards less rainy days with more precipitation events and a lower intensity on average. Consequently, water balance decreased, although evapotranspiration also decreased, mainly in summer and spring. This trend is likely rooted in a rising vapor pressure deficit, due to rising temperature. This limits evapotranspiration in high radiation conditions, because of a rise in stomatal resistance. Against expectations, extreme precipitation reduced in volume and intensity over the observation period, which was evident in precipitation indices and sub-daily analysis. Subdaily analysis and event-based analysis of precipitation proved to be insightful when determining extreme precipitation trends. However, sub-daily analysis would not have been necessary for this case to detect extreme precipitation trends. This may be site-specific, as for Bayreuth, indices and sub-daily analysis were not in total agreement. As a consequence, drought stress could significantly increase in the future, as the water table lowers and water availability decreases in the growing season. More evenly distributed precipitation, because of a decrease in extreme precipitation, may aid vegetation in coping with a rise in drought stress.

The main limitation of this study was the statistical significance of trends because of precipitations' high temporal variability. A fair number of the observed trends do not hold their significance when the observation period was shortened by a couple of years. Therefore, this study should be repeated in the future, to determine, whether the trends were mainly based on the observation period. Further research should be carried out to establish the changes that weather systems have gone through in this period, as this could be the cause of the observed trends in precipitation and extreme precipitation. These findings should be compared in depth to nearby stations like Bayreuth, to investigate how topography impacts precipitation and extreme precipitation trends.

References

Myles R. Allen and William J. Ingram. Constraints on future changes in climate and the hydrologic cycle. *Nature*, 419(6903):224–232, 2002. doi: 10.1038/nature01092.

Martin Beniston, Daniel Farinotti, Markus Stoffel, Liss M. Andreassen, Erika Coppola, Nicolas Eckert, Adriano Fantini, Florie Giacona, Christian Hauck, Matthias Huss, Hendrik Huwald, Michael Lehning, Juan-Ignacio López-Moreno, Jan Magnusson, Christoph Marty, Enrique Morán-Tejéda, Samuel Morin, Mohamed Naaim, Antonello Provenzale, Antoine Rabatel, Delphine Six, Johann Stötter, Ulrich Strasser, Silvia Terzago, and Christian Vincent. The european mountain cryosphere: a review of its current state, trends, and future challenges. *The Cryosphere*, 12(2):759–794, 2018. doi: 10.5194/tc-12-759-2018.

A. Casanueva, C. Rodríguez-Puebla, M. D. Frías, and N. González-Reviriego. Variability of extreme precipitation over europe and its relationships with teleconnection patterns. *Hydrology and Earth System Sciences*, 18(2):709–725, 2014. doi: 10.5194/hess-18-709-2014.

M. Collins, Reto Knutti, Julie Arblaser, Jean-Louis Dufresne, Thierry Fichefet, Pierre Friedlingstein, Xuejie Gao, William Gutowski, Tim Johns, Gerhard Krinner, Mxolisi Shongwe, Claudia Teballdi, Andrew Weaver, and Michael Wehner. Long-term climate change: Projections, commitments and irreversibility. *IPCC*, pages 1029–1136, 2013.

Robert J. H. Dunn, Lisa V. Alexander, Markus G. Donat, Xuebin Zhang, Margot Bador, Nicholas Herold, Tanya Lippmann, Rob Allan, Enric Aguilar, Abdoul Aziz Barry, Manola Brunet, John Caesar, Guillaume Chagnaud, Vincent Cheng, Thelma Cinco, Imke Durre, Rosaline Guzman, Tin Mar Htay, Wan Maisarah Wan Ibadullah, Muhammad Khairul Izzat Bin Ibrahim, Mahbobeh Khoshkam, Andries Kruger, Hisayuki Kubota, Tan Wee Leng, Gerald Lim, Lim Li-Sha, Jose Marengo, Sifiso Mbatha, Simon McGree, Matthew Menne, Maria Milagros Skansi, Sandile Ngwenya, Francis Nkrumah, Chalump Oonariya, Jose Daniel Pabon-Caicedo, Gérémy Panthou, Cham Pham, Fatemeh Rahimzadeh, Andrea Ramos, Ernesto Salgado, Jim Salinger, Youssouph Sané, Ardhasena Sopaheluwakan, Arvind Srivastava, Ying Sun, Bertrand Timbal, Nichanun Trachow, Blair Trewin, Gerard Schrier, Jorge Vazquez-Aguirre, Ricardo Vasquez, Claudia Villarroel, Lucie Vincent, Theo Vischel, Russ Vose, and Mohd Noor'Arifin Bin Hj Yussof. Development of an updated global land in situ–based data set of temperature and precipitation extremes: Hadex3. *Journal of Geophysical Research: Atmospheres*, 125(16), 2020. ISSN 2169897X. doi: 10.1029/2019JD032263.

Thomas Foken. Lufthygienisch-bioklimatische aufzeichnungen des oberen egertales. 2003.

Thomas Foken. Das klima von bayreuth. *Standort*, 31(3):150–152, 2007. ISSN 1432-220X. doi: 10.1007/s00548-007-0045-x.

Thomas Foken and Johannes Lüers. Regionale atmosphärische prozesse und ihre raumzeitliche ausprägung. *Annalen der Meteorologie*, 8(46):25–29, 2013.

Thomas Foken and Johannes Lüers. Regionale ausprägung des klimawandels in oberfranken. In Gabriele Obermaier and Cyrus Samimi, editors, *Folgen des Klimawandels*, volume 8 of *Bayreuther Kontaktstudium Geographie*, pages 33–43. Verlag Naturwissenschaftliche Gesellschaft Bayreuth e.V, Bayreuth, 2015. ISBN 978-3-939146-21-6.

Eunice Foote. Circumstances affecting the heat of the sun's rays. (22):382–383, 1856.

Franziska Schwab. *Auswirkungen der Dürresommer 2018 und 2019 auf den Kohlenstoff- und Wasserhaushalt eines Fichtenwaldes*. PhD thesis, Universität Bayreuth, Abteilung Mikrometeorologie, Bayreuth, 2021.

M. Georgescu, A. M. Broadbent, M. Wang, E. Scott Krayenhoff, and M. Moustaoui. Precipitation response to climate change and urban development over the continental united states. *Environmental Research Letters*, 16(4):044001, 2021. doi: 10.1088/1748-9326/abd8ac.

Fausto Guzzetti, Colin Stark, and Paola Salvati. Evaluation of flood and landslide risk to the population of italy. *Environmental Management*, 36:15–36, 08 2005. doi: 10.1007/s00267-003-0257-1.

Samuli Helama, Kristina Sohar, Alar Läänelaid, Szymon Bijak, and Jaak Jaagus. Reconstruction of precipitation variability in estonia since the eighteenth century, inferred from oak and spruce tree rings. *Climate Dynamics*, 50(11-12):4083–4101, 2018. ISSN 0930-7575. doi: 10.1007/s00382-017-3862-z.

Charles D. Keeling, Robert B. Bacastow, Arnold E. Bainbridge, Carl A. Ekdahl, Peter R. Guenther, Lee S. Waterman, and John F. S. Chin. Atmospheric carbon dioxide variations at mauna loa observatory, hawaii. *Tellus*, 28(6):538–551, 1976. ISSN 00402826. doi: 10.1111/j.2153-3490.1976.tb00701.x.

Alan K. Knapp, Philip A. Fay, John M. Blair, Scott L. Collins, Melinda D. Smith, Jonathan D. Carlisle, Christopher W. Harper, Brett T. Danner, Michelle S. Lett, and James K. McCarron. Rainfall variability, carbon cycling, and plant species diversity in a mesic grassland. *Science*, 298(5601):2202–2205, 2002. doi: 10.1126/science.1076347.

M. Latif and T. P. Barnett. Causes of decadal climate variability over the north pacific and north america. *Science*, 266(5185):634–637, 1994. doi: 10.1126/science.266.5185.634.

Leila Schuh. *Regional climate regulation by different land cover types: comparing homogeneous and heterogeneous structures in agricultural landscapes*. 2017.

Gunnar Lischeid, Sven Frei, Bernd Huwe, Christina Bogner, Johannes Lüers, Wolfgang Babel, and Thomas Foken. *Catchment Evapotranspiration and Runoff*, pages 355–375. 03 2017. ISBN 978-3-319-49387-9. doi: 10.1007/978-3-319-49389-3$_1$5.

Johannes Lüers, Barbara Grasse, Thomas Wrzesinsky, and Thomas Foken. Climate, air pollutants, and wet deposition. In Thomas Foken, editor, *Energy and Matter Fluxes of a Spruce Forest Ecosystem*, pages 41–72. Springer International Publishing, Cham, 2017. ISBN 978-3-319-49389-3. doi: 10.1007/978-3-319-49389-3_3.

Ewa Łupikasza. Definitions and indices of precipitation extremes. In Ewa Łupikasza, editor, *The Climatology of Air-Mass and Frontal Extreme Precipitation*, Springer Atmospheric Sciences, pages 39–82. Springer International Publishing, Cham, 2016. ISBN 978-3-319-31476-1. doi: 10.1007/978-3-319-31478-5_2.

T. J. Osborn, P. D. Jones, D. H. Lister, C. P. Morice, I. R. Simpson, J. P. Winn, E. Hogan, and I. C. Harris. Land surface air temperature variations across the globe updated to 2019: The crutem5 data set. *Journal of Geophysical Research: Atmospheres*, 126(2), 2021. ISSN 2169897X. doi: 10.1029/2019JD032352.

P. Pall, M. R. Allen, and D. A. Stone. Testing the clausius–clapeyron constraint on changes in extreme precipitation under co2 warming. *Climate Dynamics*, 28(4):351–363, 2007. ISSN 0930-7575. doi: 10.1007/s00382-006-0180-2.

Cynthia Rosenzweig, David Karoly, Marta Vicarelli, Peter Neofotis, Qigang Wu, Gino Casassa, Annette Menzel, Terry L. Root, Nicole Estrella, Bernard Seguin, Piotr Tryjanowski, Chunzhen Liu, Samuel Rawlins, and Anton Imeson. Attributing physical and biological impacts to anthropogenic climate change. *Nature*, 453(7193):353–357, 2008. doi: 10.1038/nature06937.

Jacob Scheff and Dargan M. W. Frierson. Scaling potential evapotranspiration with greenhouse warming. *Journal of Climate*, 27(4):1539–1558, 2014. ISSN 0894-8755. doi: 10.1175/JCLI-D-13-00233.1.

Andrew Schurer, Andrew Ballinger, Andrew Friedman, and Gabriele Hegerl. Human influence strengthens the contrast between tropical wet and dry regions. *Environmental Research Letters*, 15, 10 2020. doi: 10.1088/1748-9326/ab83ab.

Thomas Stocker, editor. *Climate change 2013: The physical science basis ; Working Group I contribution to the Fifth Assessment Report of the Intergovernmental Panel on Climate Change*. Cambridge Univ. Press, New York, NY, 2014. ISBN 110766182X.

Chung-Hsiung Sui, Masaki Satoh, and Kentaroh Suzuki. Precipitation efficiency and its role in cloud-radiative feedbacks to climate variabilityprecipitation efficiency and its role in cloud-radiative feedbacks to climate variability. *Journal of the Meteorological Society of Japan. Ser. II*, 98, 03 2020. doi: 10.2151/jmsj.2020-024.

Qiaohong Sun, Xuebin Zhang, Francis Zwiers, Seth Westra, and Lisa V. Alexander. A global, continental, and regional analysis of changes in extreme precipitation. *Journal of Climate*, 34(1):243–258, 2021. ISSN 0894-8755. doi: 10.1175/JCLI-D-19-0892.1.

K. E. Trenberth. Changes in precipitation with climate change. *Climate Research*, 47(1): 123–138, 2011. ISSN 0936-577X. doi: 10.3354/cr00953.

Kevin E. Trenberth, Aiguo Dai, Roy M. Rasmussen, and David B. Parsons. The changing character of precipitation. *Bulletin of the American Meteorological Society*, 84(9):1205–1218, 2003. ISSN 0003-0007. doi: 10.1175/BAMS-84-9-1205.

John Tyndall. I. the bakerian lecture.—on the absorption and radiation of heat by gases and vapours, and on the physical connexion of radiation, absorption, and conduction. *Philosophical Transactions of the Royal Society of London*, 151:1–36, 1861. ISSN 0261-0523. doi: 10.1098/rstl.1861.0001.

E. J. M. van den Besselaar, A. M. G. Klein Tank, and T. A. Buishand. Trends in european precipitation extremes over 1951-2010. *International Journal of Climatology*, pages n/a–n/a, 2012. ISSN 0899-8418. doi: 10.1002/joc.3619.

Jordi Vilà-Guerau de Arellano. *Atmospheric Boundary Layer: Integrating Air Chemistry and Land Interactions*. Cambridge Univ Press, Cambridge, 2015. ISBN 1107090946. doi: 10.1017/CBO9781316117422.

Wenxia Zhang and Tianjun Zhou. Increasing impacts from extreme precipitation on population over china with global warming. *Science Bulletin*, 65, 12 2019. doi: 10.1016/j.scib.2019.12.002.

Declaration of Authorship

I hereby confirm that this thesis and the work presented in it is entirely my own. Where I have consulted the work of others this is always clearly stated. All statements taken literally from other writings or referred to by analogy are marked and the source is always given. This paper has not yet been submitted to another examination office, either in the same or similar form. This work does not claim to be complete.

Place, Date Signature

Appendix

R Functions

```
# calculate stomatal resistance after Noilhan and Planton (1989) = Jarvis scheme
rs.NP = function(SWD, SM, tair, rH, RGL=90, LAI, SRMIN, SRMAX = 2500,
ETAWI, ETAFC)


    # all parameter can be a single number of a vector of length(SWD)
# SWD: short-wave downwelling radiation in Wm-2
# SM: volumetric soil moisture in m3/m3
# RGL: lower radiation limit in Wm-2
# LAI: leaf area index in m2/m2
# SRMIN: minimum stomata resistance in s/m
# SRMAX: maximum stomata resistance in s/m
# ETAWI: volumetric soil moisture at wilting point in m3/m3
# ETAFC: volumetric soil moisture at field capacity in m3/m3
SWD[SWD < 0] = 0
#F1:
## Jarvis-Stewart approach as used in the class model (see book, chapter 9. p.123)
##NP89 with RGL = 90, LAI = 2 and Rsmin = 60
F1 = pmax(1,0.81*(0.004*SWD+1)/(0.004*SWD+0.05))
# F2 (amount of water transpired not taken into account here,
# as forced by measured soil moisture)
F2 = (SM-ETAWI)/(ETAFC-ETAWI)
F2[SM > ETAFC] = 1
F2[SM < ETAWI] = 0

# F3: Cheeting! using air temperature instead of surface temperature
F3= exp(-gD*VPD)
F3[F3 <= 0] = SRMIN/SRMAX
F3[F3 > 1] = 1

F4= 1-0.0016*(298.-tair-273.15)^2
F4[F4 <= 0] = SRMIN/SRMAX

RS = SRMIN*F1/F2/F3/F4
RS[RS > SRMAX] = SRMAX
return(RS)
```

```
    PM = function(Qa,t,u,q,p, LAI, CH, rs.i, ...)
# calculate Penman-Monteith equation
# Qa: available energy (Wm-2)
# t: air temperature (degC)
# u: wind velocity at zm (ms-1)
# hum: air humidity, as specific humidity in kgkg-1 (which.hum="q")
# or as vapour pressure in hPa (which.hum="e")
# or as relative humidity in percent (which.hum="rH")
# p: air pressure (hPa)
# LAI: leaf area index (m3m-3)
# CH: Bulk coefficient (stanton number)
# rs.i: stomata resistance of a single leaf

# constants
cp = 1004.67 # J kg-1 K-1
Ra = 287.0586 # specific gas constant for dry air J kg-1 K-1
lambda = ( 2.501 - 0.00237*t ) *1000000 # J kg-1
Tv = (1 + 0.608 * q) * (t+273.15)
rho = p*100/(Ra * Tv)
Esat = Magnus(t,...)
qsat = 0.622 * Esat / (p - 0.378 * Esat)

gamma = cp/lambda
sc = 0.622* qsat* lambda/(Ra * (t+273.15)^2)
ra = 1/(CH*u)
rs = rs.i / (LAI*0.5)

Qh = (gamma*Qa*(1+rs/ra) - rho*cp*(qsat-q)/ra) /(sc+gamma*
(1+rs/ra))
Qe = (sc*Qa + rho*cp*(qsat-q)/ra) /(sc+gamma*(1+rs/ra))

ETa = Qe * 24*3600/lambda
return(cbind(ETa, ra, rs))]
```

Figures

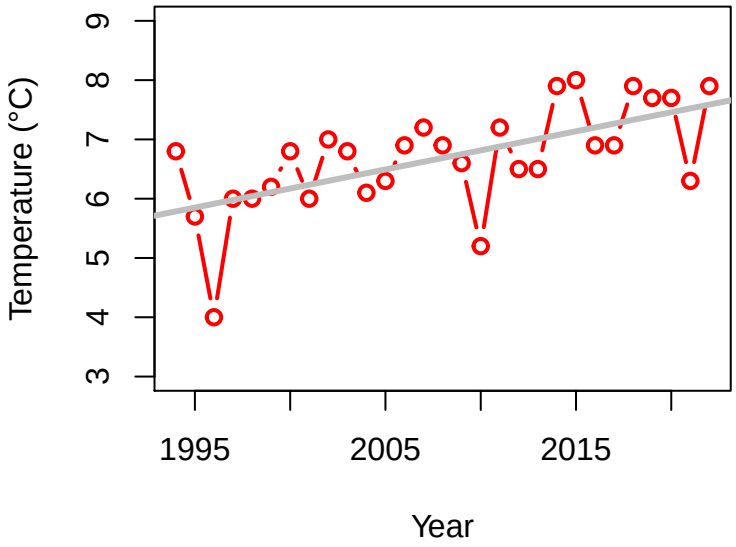

Figure 24: Annual mean temperature. (trend: p=0.0003, m=0.06).

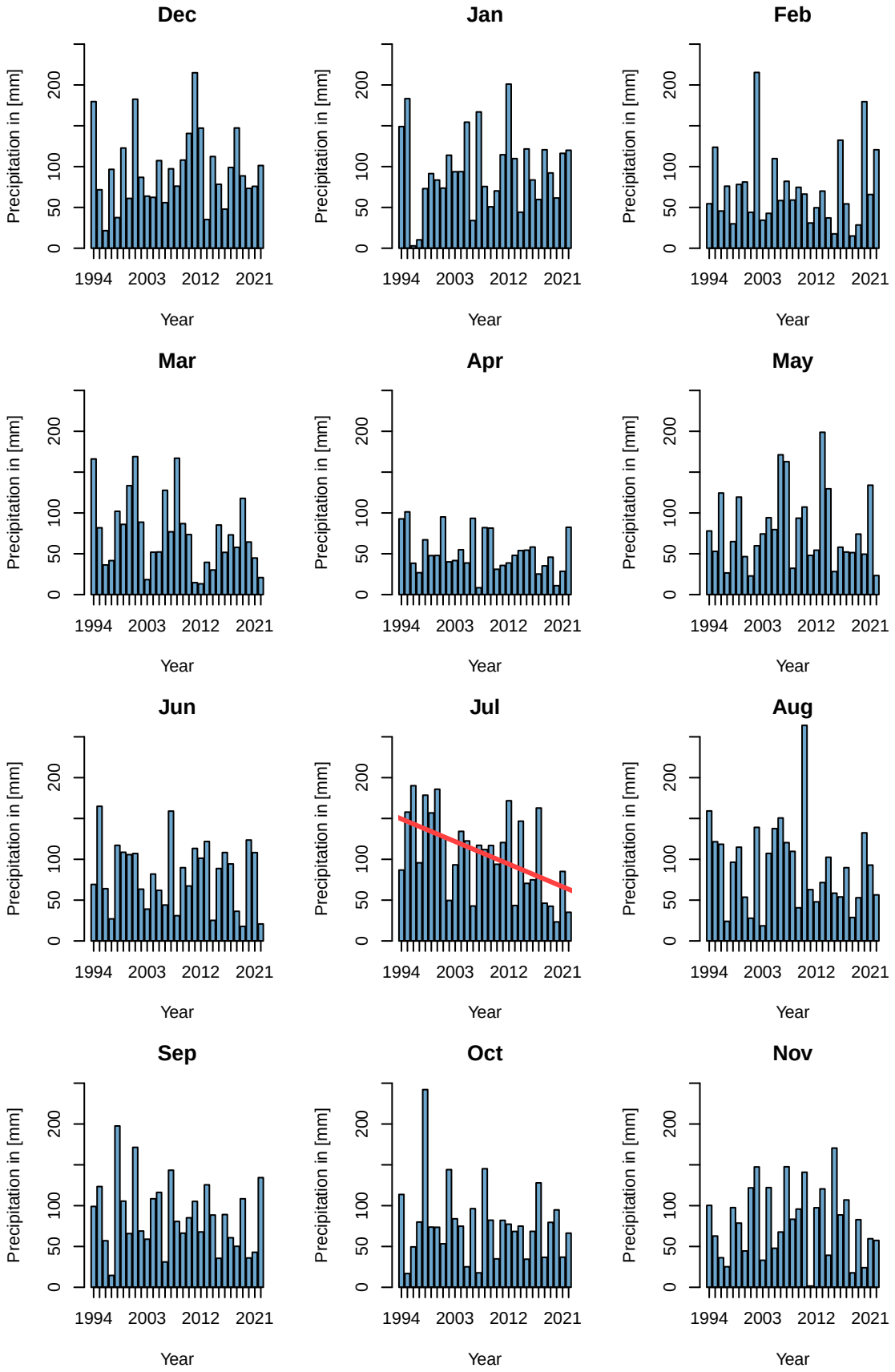

Figure 25: Monthly precipitation. (summer trend: p=0.002, m=-3.0)

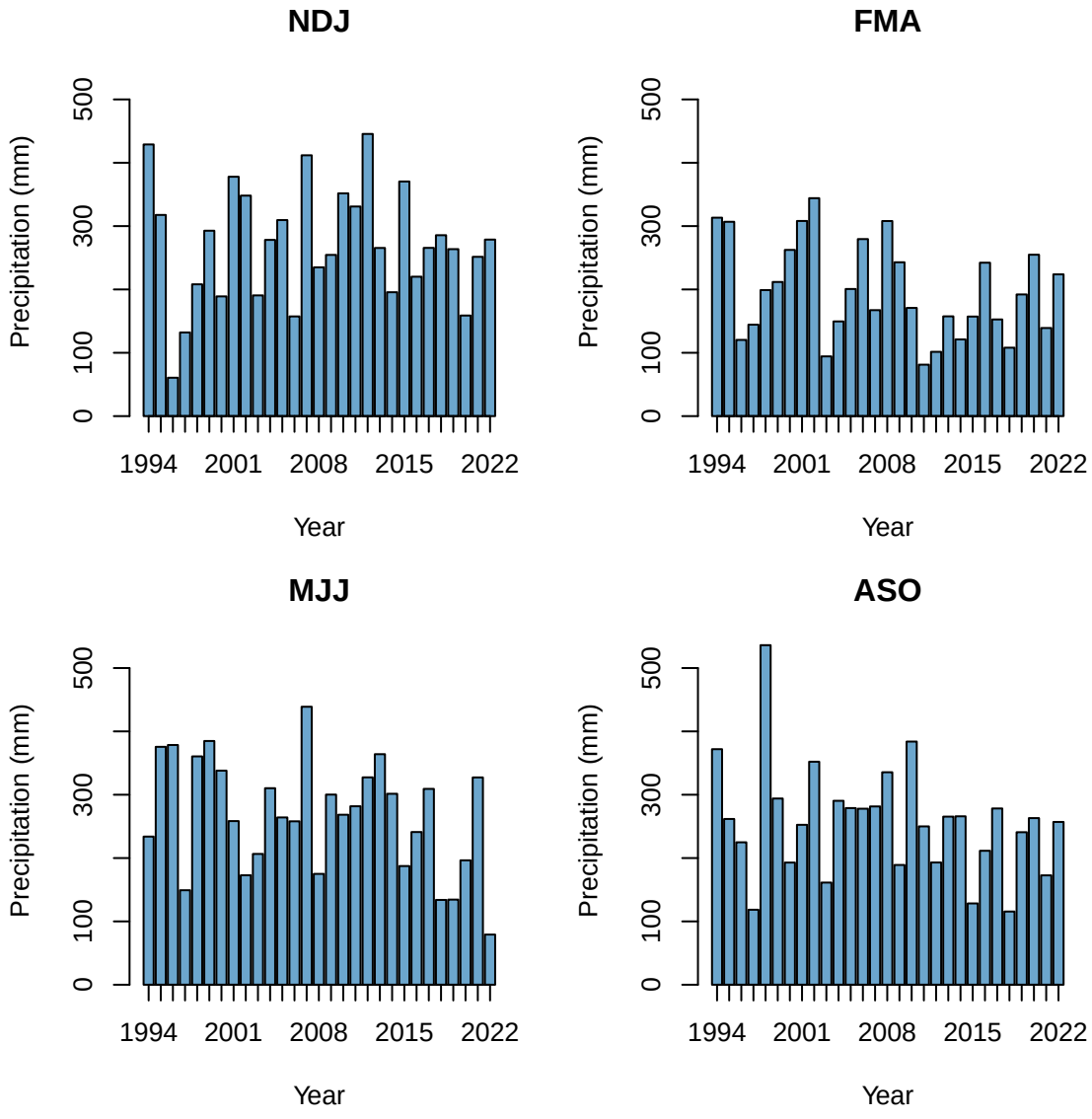

Figure 26: Hydrological seasonal precipitation.

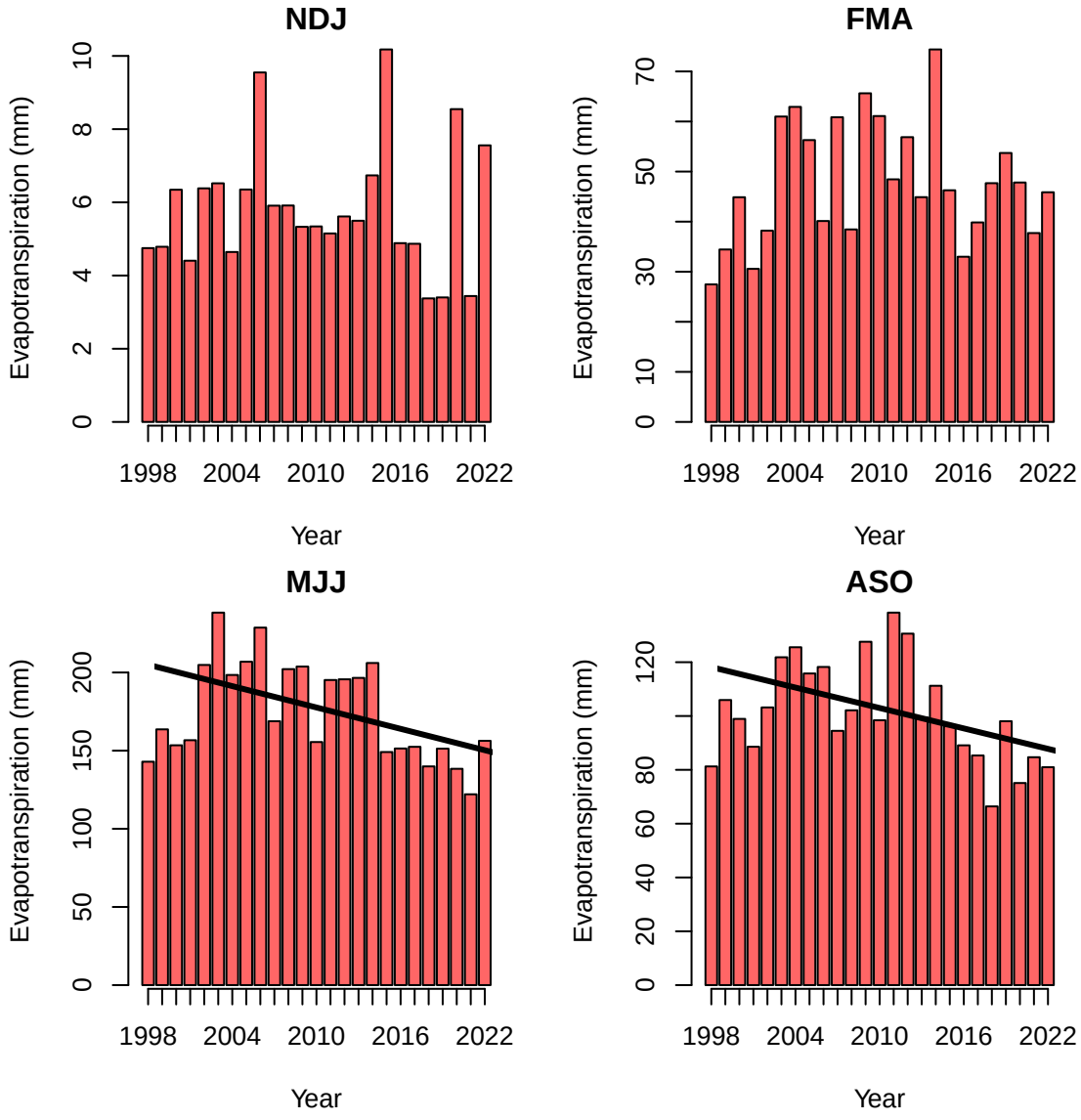

Figure 27: Hydrological seasonal evapotranspiration. (trend summer: p=0.025, m=-2.27 , trend autumn: p=0.046, m=-1.16)

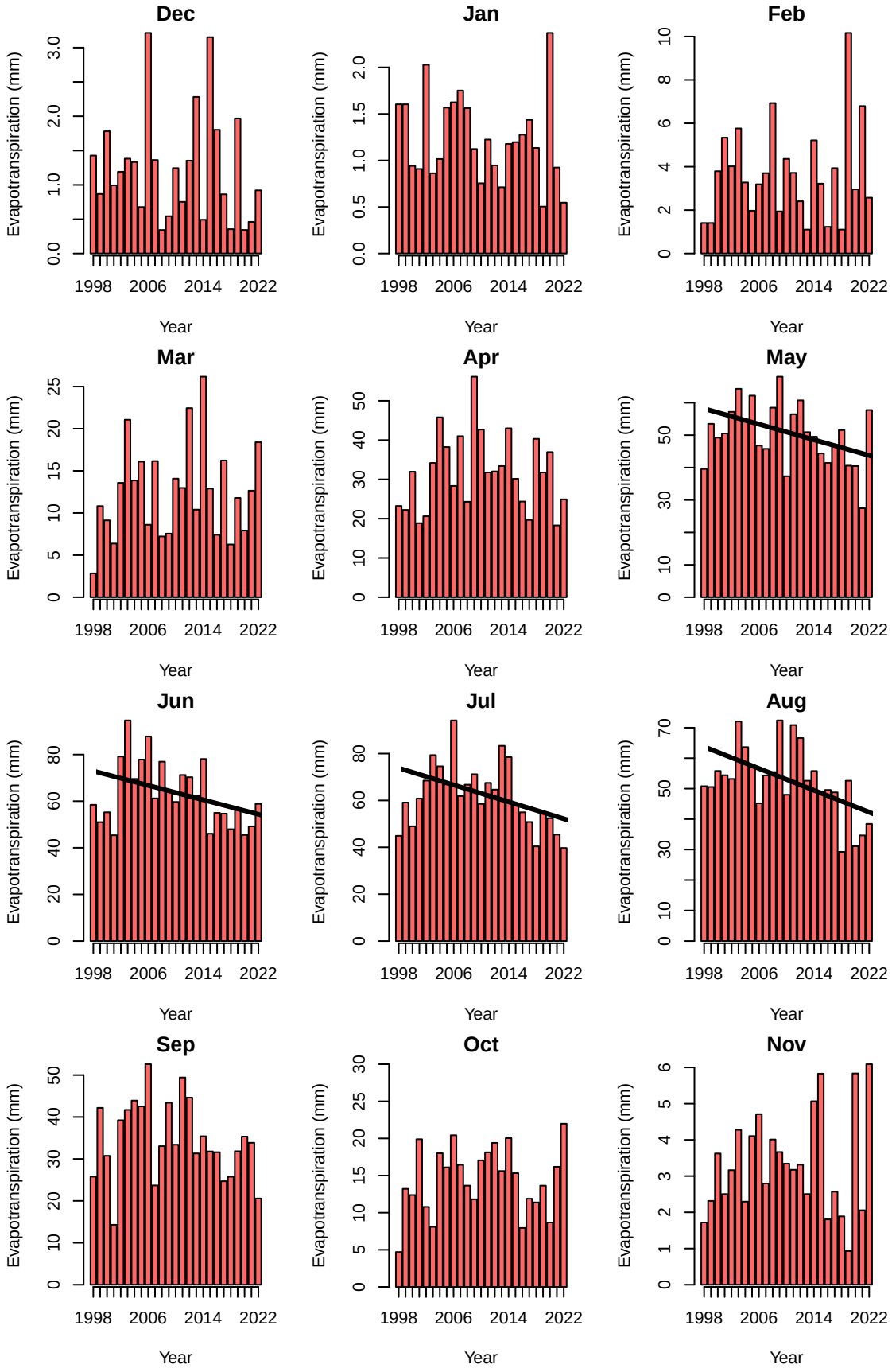

Figure 28: Monthly evapotranspiration. (trend May: p=0.03, m=-0.6, trend June: p=0.049, m=-0.77, trend July: p=0.009, m=-0.90, trend August: p=0.009, m=-0.89)

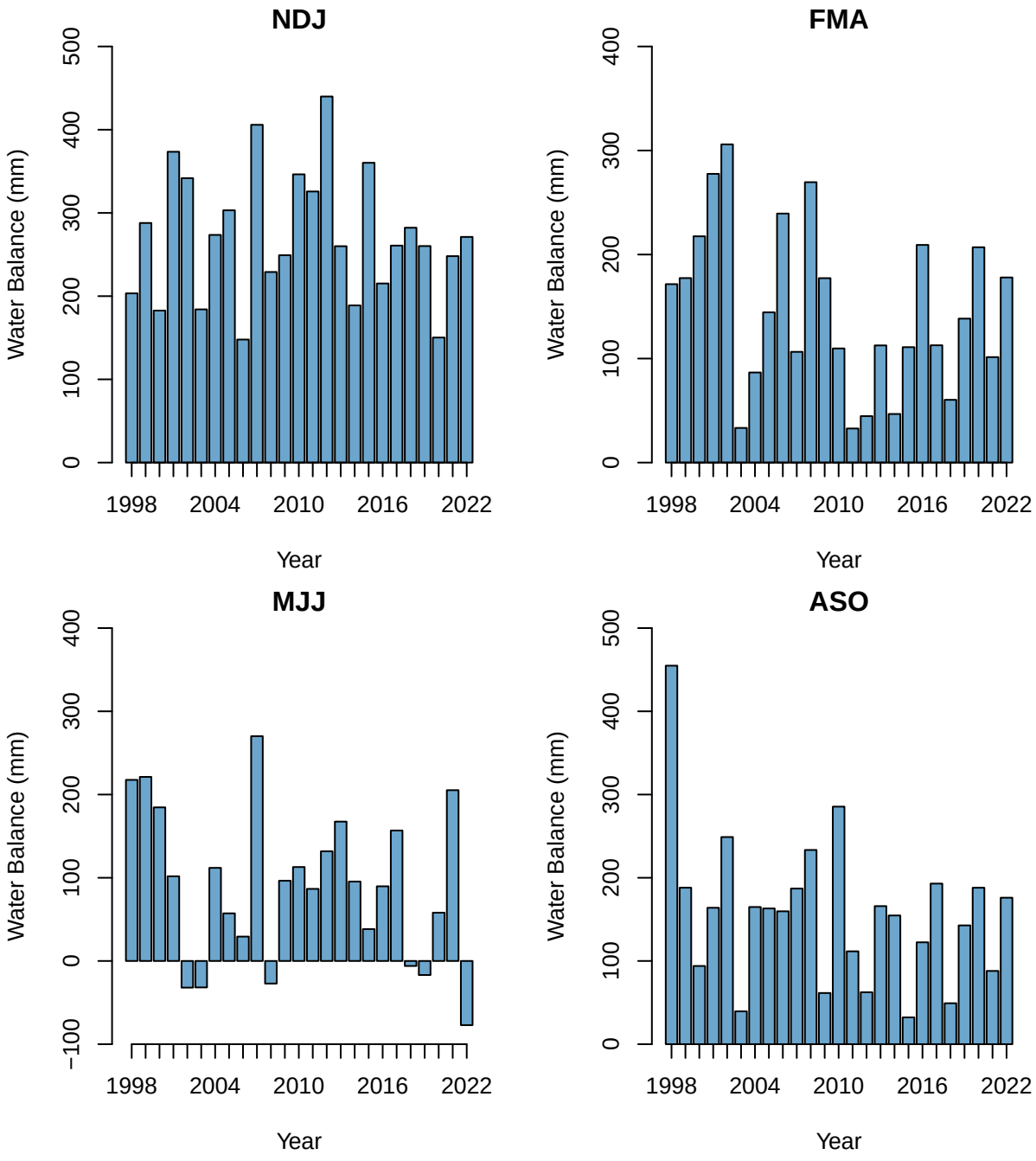

Figure 29: Hydrological seasonal water balance.

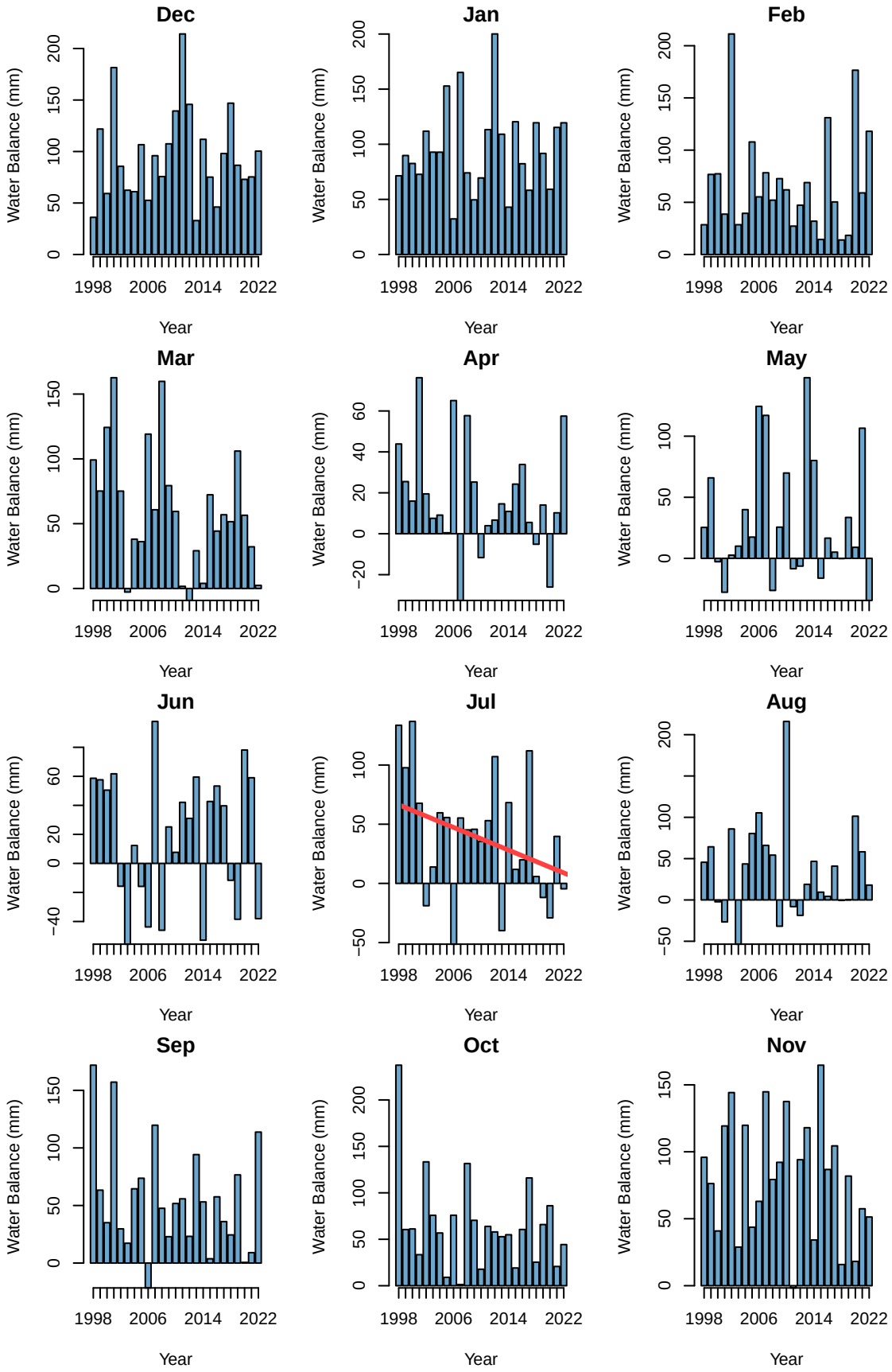

Figure 30: Monthly water balance. (trend July: p=0.049, m=-2.39)

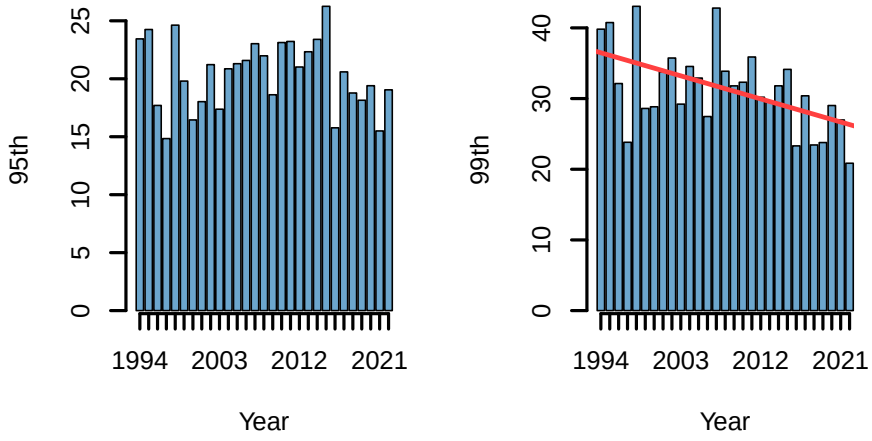

Figure 31: Yearly 95th precipitation percentile (left) and 99th precipitation percentile (right) of daily precipitation. (99th trend: p=0.006, m=-0.36).

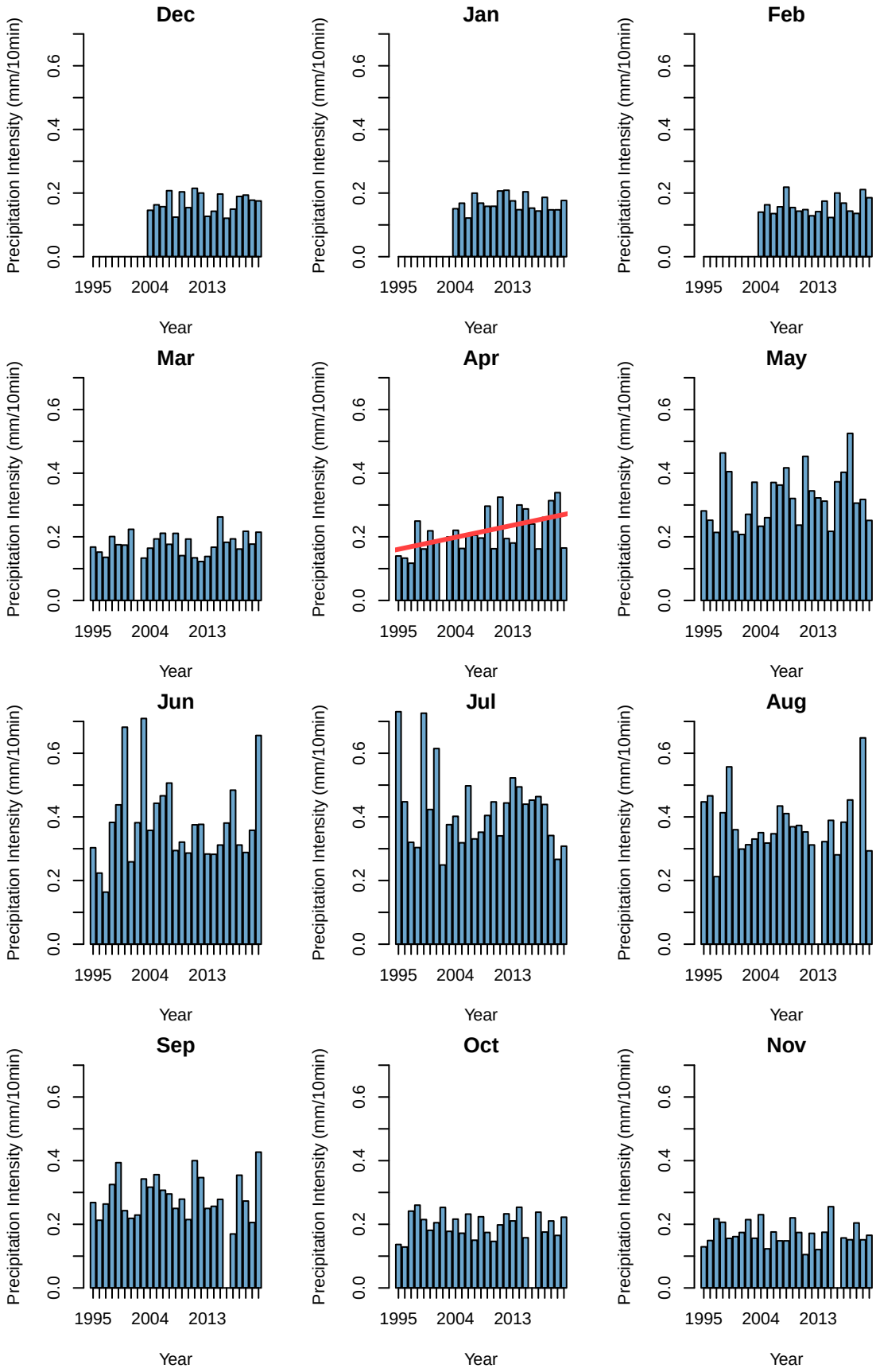

Figure 32: Monthly averages of precipitation intensity. (April trend: p=0.014, m=0.004)

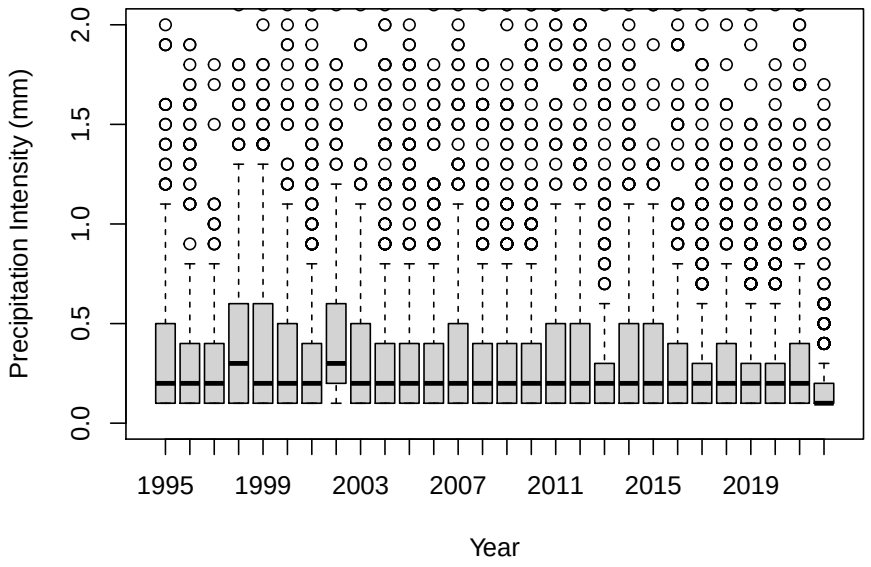

Figure 33: Maximum event intensity distribution per year.

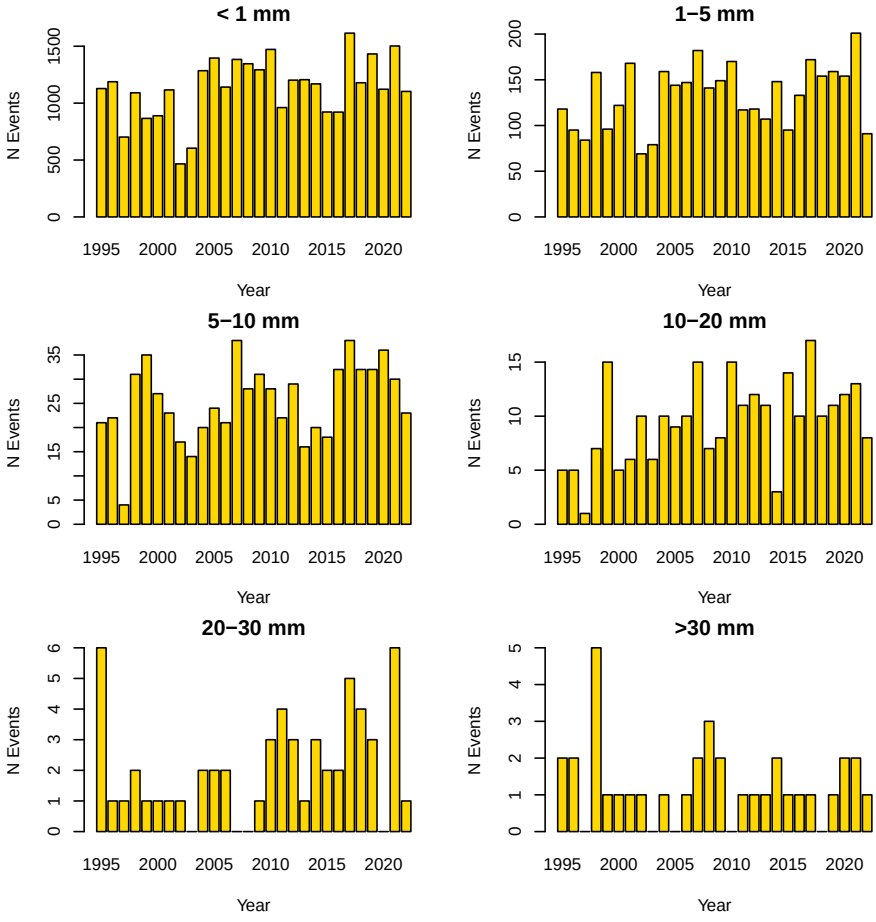

Figure 34: Number of events with event precipitation sum below 1 mm, 1-5 mm, 5-10 mm, 10-20 mm, 20-30 mm and above 30 mm. No trends for 2004-2022.

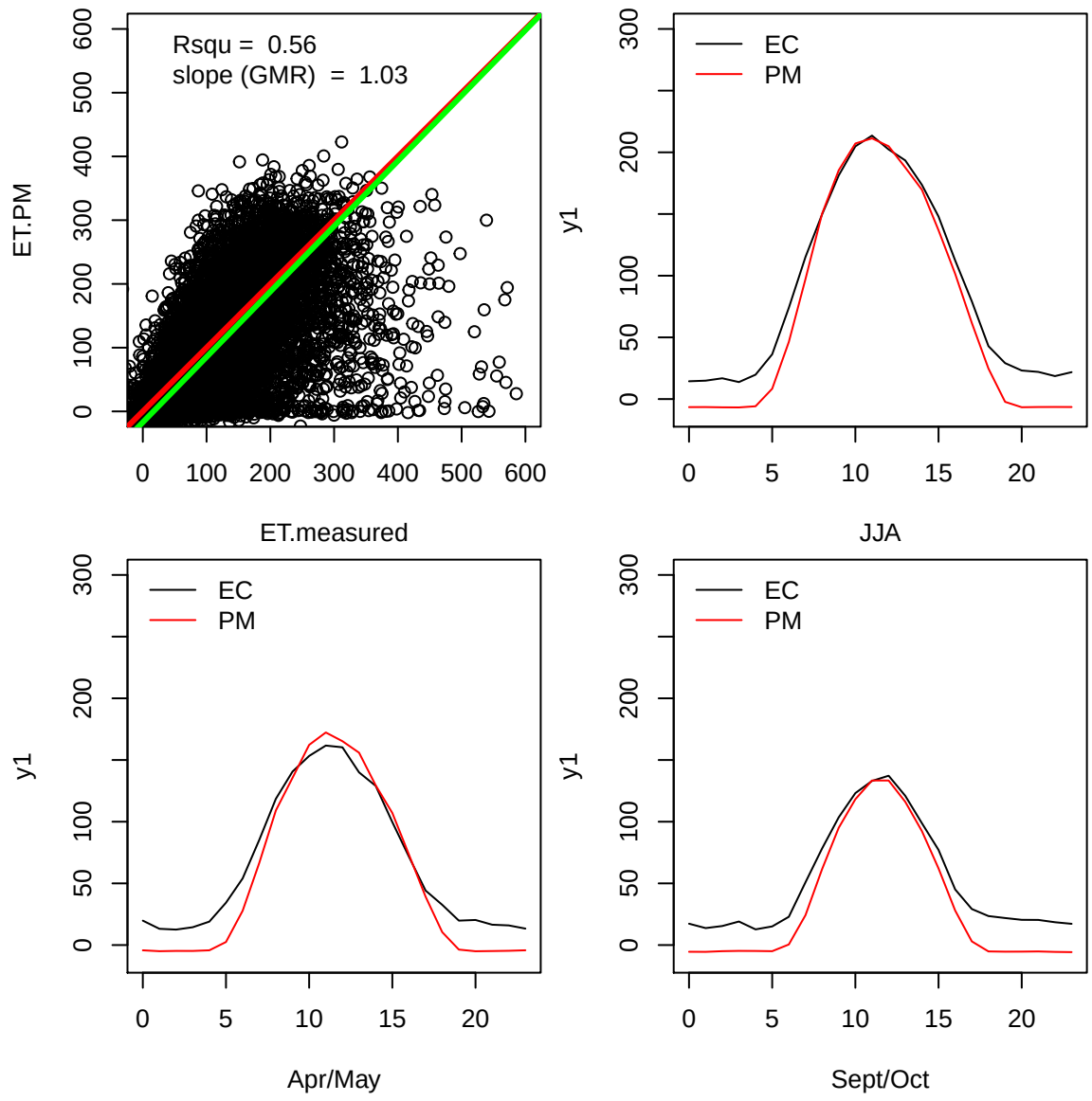

Figure 35: Validation of Penman Monteith Model with Eddy-Covariance data with diurnal means of seasons and months.

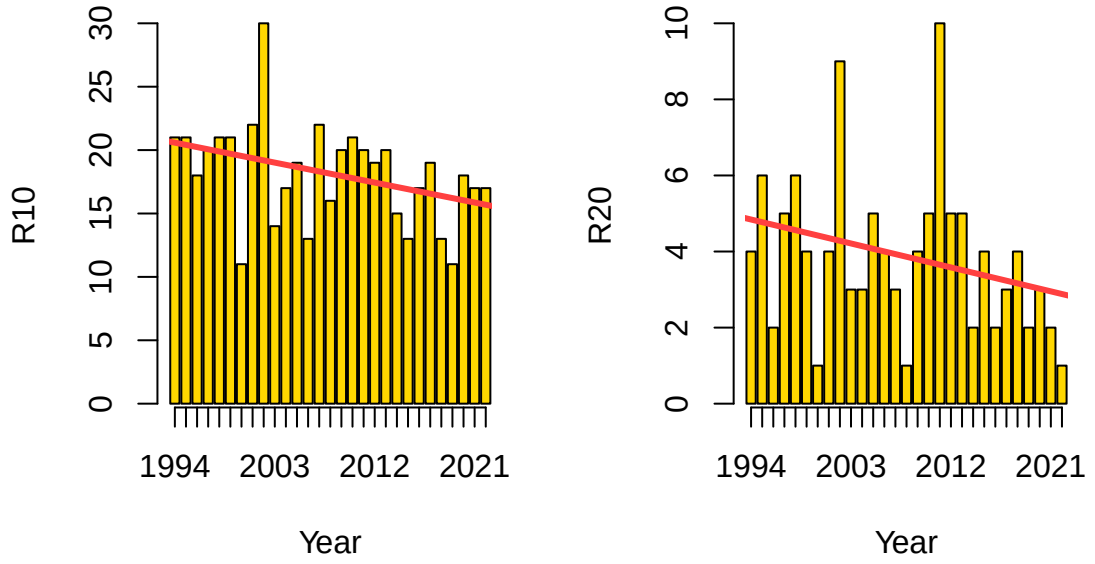

Figure 36: Bayreuth: Number of precipitation days with more then 10 mm of precipitation (left) and 20 mm of precipitation (right) with statistically significant trends.

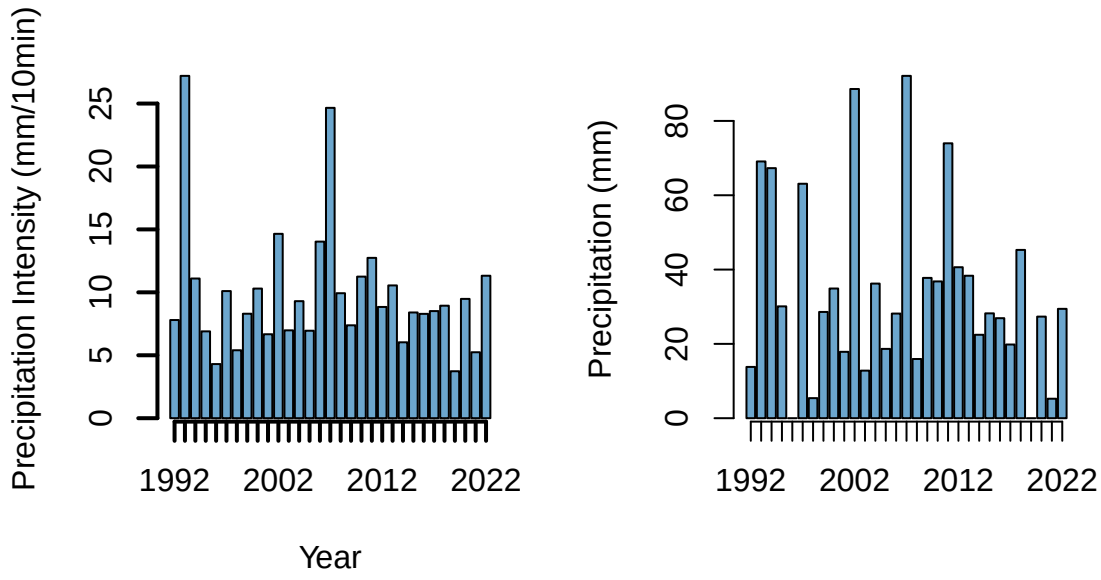

Figure 37: Bayreuth: Maximum precipitation intensity for each year (left) and precipitation with intensity greater then 5 mm fallen in a year (right)

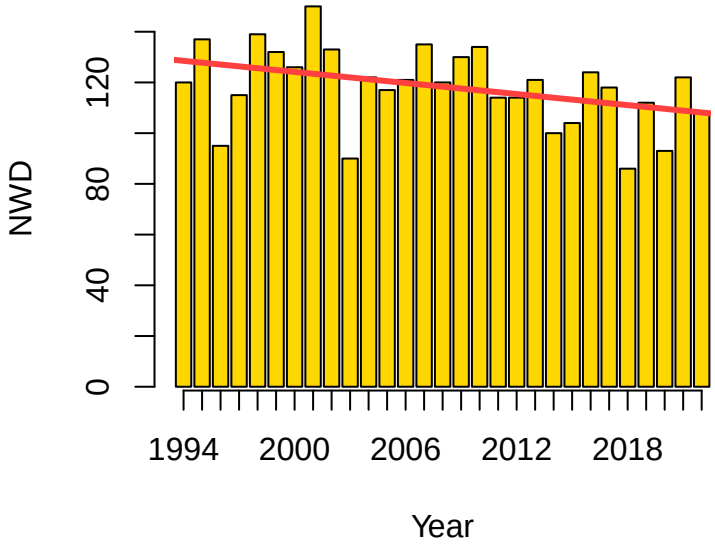

Figure 38: Bayreuth: number of wet days per year with significantly decreasing trend.

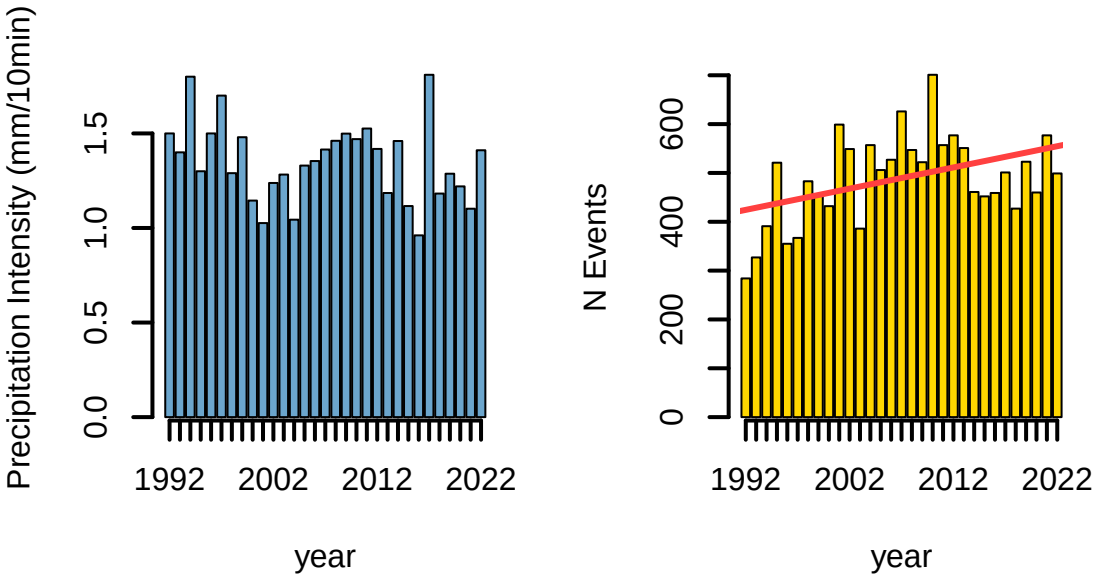

Figure 39: Bayreuth: 95th percentile of precipitation intensity (left) and number of events per year (right) with a significant trend.